



HAL
open science

A new species of *Halisaurus* (Mosasauridae: Halisaurinae) from the lower Maastrichtian (Upper Cretaceous) of the Western Desert, Egypt

Ahmed A Shaker, Nicholas R Longrich, Amin Strougo, Anhar Asan, Nathalie Bardet, Mohamed K Mousa, Abdel Aziz Tantawy, Gebely A Abu El-Kheir

► To cite this version:

Ahmed A Shaker, Nicholas R Longrich, Amin Strougo, Anhar Asan, Nathalie Bardet, et al.. A new species of *Halisaurus* (Mosasauridae: Halisaurinae) from the lower Maastrichtian (Upper Cretaceous) of the Western Desert, Egypt. *Cretaceous Research*, 2024, 154, pp.105719. 10.1016/j.cretres.2023.105719 . hal-04719061

HAL Id: hal-04719061

<https://hal.science/hal-04719061v1>

Submitted on 8 Oct 2024

HAL is a multi-disciplinary open access archive for the deposit and dissemination of scientific research documents, whether they are published or not. The documents may come from teaching and research institutions in France or abroad, or from public or private research centers.

L'archive ouverte pluridisciplinaire **HAL**, est destinée au dépôt et à la diffusion de documents scientifiques de niveau recherche, publiés ou non, émanant des établissements d'enseignement et de recherche français ou étrangers, des laboratoires publics ou privés.

1 **A new species of *Halisaurus* (Mosasauridae: Halisaurinae)**
2 **from the lower Maastrichtian (**Upper** Cretaceous) of the**
3 **Western Desert, Egypt**

4
5 **Ahmed A. Shaker^a, Nicholas R. Longrich^{b*}, Amin Strougo^a, Anhar Asan^a, Nathalie Bardet^c, Mohamed K.**
6 **Mousa^d, Abdel Aziz Tantawy^d, Gebely A. Abu El-Kheir^d.**

7
8 ^aDepartment of Geology, Faculty of Science, Ain Shams University, 11566 Cairo, Egypt

9 ^bDepartment of Biology and Biochemistry, University of Bath, Claverton Down, Bath, BA2 7AY United Kingdom

10 ^cCR2P, Centre de Recherche en Paléontologie – Paris, Muséum National d’Histoire Naturelle, CP38, 57 Rue Cuvier,
11 75005 Paris, France

12 ^dNew Valley Vertebrate Palaeontology Centre, New Valley University, New Valley, Egypt

13
14 *email: nrl22@bath.ac.uk

15 **Keywords:** Squamata, Mosasauridae, Halisaurinae, Late Cretaceous, Paleobiogeography, Tethys.

16 A B S T R A C T

17

18 Mosasaurids were highly diverse and dominant as predators in late Cretaceous marine
19 ecosystems. In the Maastrichtian, the Halisaurinae, a clade of relatively small-bodied
20 mosasaurids, became common, especially in North Africa. Here, we report a new species of
21 halisaurine from the lower Maastrichtian Dakhla Shale of the Western Desert of Egypt.
22 *Halisaurus hebae* sp. nov. resembles *Halisaurus platyspondylus* and *H. arambourgi* in the shape
23 of the frontal, suggesting close affinity with those species. A revised halisaurine phylogeny
24 shows a cluster of species characterized by modification of the orbital bones to accommodate
25 large eyes, suggesting a shift towards the use of visual cues to find prey, perhaps in low light
26 conditions. The abundance and diversity of halisaurines in Africa contrasts with their relative
27 rarity elsewhere in the world, emphasizing the regionalization of marine reptile faunas in the
28 Maastrichtian.

29

30 **1. Introduction**

31 In recent years, several paleontological expeditions have been undertaken in the Dakhla basin of
32 the Western Desert of Egypt in collaboration with Egyptian universities, following the
33 establishment of the Vertebrate Paleontology Center in 2020 at the University of the New
34 Valley, Kharga city. The field work so far has resulted in the discovery of great numbers of
35 vertebrate remains. These include marine reptiles such as plesiosaurs, mosasaurids, and turtles,
36 as well as crocodiles, dinosaurs, and also a variety of bony fish and chondrichthyan remains,
37 especially teeth, from Campanian and Maastrichtian strata (AbdelGawad et al., 2021; Abu El-
38 Kheir et al., 2021; Abu El-Kheir et al., 2022; Capasso et al., 2021). The main vertebrate-bearing
39 horizons are the Quseir Variegated **Shales** and Duwi Formation, of Campanian age, and the
40 Dakhla Shale, of Maastrichtian to Paleocene age (see Geographical and Stratigraphic Settings,
41 below).

42 Fossils of the mosasaurid subfamily Halisaurinae Bardet and Pereda Suberbiola, 2005 are
43 currently known from Santonian to upper Maastrichtian formations, and include the genera
44 *Halisaurus* (Marsh, 1869), *Phosphorosaurus* (Dollo, 1889), *Pluridens* (Lingham-Soliar, 1998)
45 and *Eonatator* Bardet and Pereda Suberbiola, 2005 (Bardet et al., 2005a; Longrich et al., 2021a).
46 *Halisaurus* is the most diverse genus. Here, we recognize four species (Table 1): *Halisaurus*
47 *platyspondylus*, *Halisaurus arambourgi*, *Halisaurus* (“*Phosphorosaurus*”) *ponpetelegans*, and
48 *Halisaurus* (“*Eonatator*”) *coellensis*. They are united by modifications to the postorbitofrontal
49 and jugal to increase the size of the orbits and binocular vision (see phylogenetic analysis,
50 below).

51 Halisaurinae exhibit a wide geographical range stretching from South and North America to
52 northern Europe, eastern Asia, northern and central Africa and the Middle East (Bardet, 2012;

53 Bardet et al., 2000; Bardet and Pereda Suberbiola, 2002; Bardet et al., 2005a; Bardet and
54 Suberbiola, 2001; Caldwell and Bell Jr, 1995; Dollo, 1889; Holmes and Sues, 2000; Konishi et
55 al., 2016; Lindgren and Siverson, 2005; Lingham-Soliar, 1991, 1996, 1998; Longrich, 2016;
56 Longrich et al., 2021a; Marsh, 1869; Páramo-Fonseca, 2013; Polcyn et al., 2012; Wiman, 1920).

57 The aim of the present work is to describe a new species of *Halisaurus*, based on a partial
58 disarticulated skeleton from the lower Maastrichtian of the Dakhla Oasis, in Egypt's Western
59 Desert.

60 2. Geographical and Stratigraphic settings

61 The specimen comes from Gebel Gifata, the type locality of the Dakhla Shale, 12 km
62 northwest of Mut, the capital of the Dakhla Oasis, located in the Western Desert of Egypt (Fig.
63 1).

64 The stratigraphic succession of Gebel Gifata exhibits three distinctive and easily
65 differentiated lithostratigraphic units, totaling about 250 m in thickness (Fig. 2). These are, in
66 ascending order, the Duwi Formation, the Dakhla Shale and the Tarawan Chalk. Several meters
67 of the Duwi Formation lie exposed at the foot of the scarp, and consist of phosphatic beds
68 alternating with dark shale. A 5 m-thick white phosphatic limestone marks the contact of the
69 Duwi Formation and the Dakhla Shale. The top of the scarp is a wall-forming, white carbonate
70 unit, about 20 m thick, forming the Tarawan Chalk. In other words, the Dakhla Shale constitutes
71 almost the entirety of the scarp face. The Dakhla Shale consists predominantly of dark gray
72 shales and mudstones, intercalated by thin- to thick-bedded light gray and brown sandstones. The
73 sandstones are usually sparsely phosphatic.

74 Stratigraphically, the contact between the Duwi and Dakhla formations coincides with the
75 boundary between planktic foraminiferal Zones CF8a/CF8b, and hence, the Campanian—

76 Maastrichtian boundary (Tantawy et al., 2001). The Cretaceous-Paleocene boundary lies within
77 the upper part of the Dakhla Shale (the upper Kharga Shale Member of some authors). It is
78 represented by 30 cm thick tan- and reddish-colored calcareous sandstone containing abundant
79 mud clasts and phosphatic nodules. The sandstone overlies an erosive, undulating surface of dark
80 gray shales. The planktic foraminifera indicate Zone P1c (Danian) as the lowest Paleocene zone,
81 overlying disconformably the upper Maastrichtian Zone CF3 (Hewaidy et al., 2017; Tantawy et
82 al., 2001).

83 Vertebrate remains occur throughout the Maastrichtian portion of the Dakhla Shale of Gebel
84 Gifata. However, three bone-bearing horizons (designated H1, H2 and H3 by Abu El-Kheir et
85 al., 2022) are particularly rich. They occur between approximately 40 and 60 m above the base
86 of the formation. These bone beds include selachians, bony fishes and reptiles, including
87 mosasaurid squamates, plesiosaurs, crocodylians and turtles. Selachians are the most abundant
88 component of the faunas, although represented by just a few species (see Abu El-Kheir et al.,
89 2022). Recently, Abu El-Kheir et al., (2022) described a new genus and species of a pycnodont
90 fish from Horizon H2, which they named *Diastemapycnodus tavernensis*. As the specific name
91 *tavernensis* was explicitly based on a personal name (in this case Louis Paul Taverne, a Belgian
92 ichthyologist), the species name of this taxon should be corrected to *Diastemapycnodus tavernei*
93 according to the recommendations of the International Code of Zoological Nomenclature.

94 Macroinvertebrates are rare in the Maastrichtian of the Dakhla Shale of Gebel Gifata. They
95 occur at many levels, and are generally well preserved as composite molds. The assemblage is
96 dominated by bivalves, but also includes ammonites and very small regular echinoids. Tantawy
97 et al. (2001) reported from the same locality a diverse array of fossils including corals,
98 gastropods, nautiloids, belemnites, and callianassids.

99 In March 2021, a partial skull and skeleton was discovered by Ahmed Shaker, Mohammed
100 Kamel and Gebely A. Abu El-Kheir, during a field trip organized by the New Valley University.
101 The fossil was embedded in a dark grey mudstone layer lying at the very base of the Dakhla
102 Shale, just above the white phosphatic limestone marking the top of the Duwi Formation. Thus
103 an earliest Maastrichtian age is assigned to it.

104 **2.2 Institutional Abbreviations** NVP: New Valley Vertebrate Paleontology Center (Kharga
105 city- New Valley Governorate-Egypt).

106 **3. Material and Methods**

107 The specimen is housed in the New Valley Vertebrate Paleontology Centre of New Valley
108 University, Kharga Oasis, New Valley governorate (Egypt), under N° NVP030. It includes
109 disarticulated isolated elements of the skull (premaxilla, maxilla, frontal, parietal, jugal, quadrate
110 and braincase) and of the mandible (dentary, splenial, coronoid, angular, surangular and
111 articular). Associated teeth and postcranial bones are represented by four cervical and four trunk
112 vertebrae. The preservation of all bones is three-dimensional (Figs. 3-13).

113 Photographs were taken using a digital camera (Af-S Nikon 24-120mm 1:4 G ED VR;
114 Nikon) and lens (Af-S Nikon 70-00 mm 1:28E FL ED VR; Nikon) in normal light.

115 **4. Systematic Paleontology**

116 Squamata Opperl, 1811

117 Mosasauridae Gervais, 1852

118 Halisaurinae Bardet and Pereda-Suberbiola, 2005

119 Halisaurini Longrich et al., 2021a

120 *Halisaurus* Marsh, 1869

121 *Halisaurus hebae* sp. nov.

122 *Holotype*. NVP030, incomplete disarticulated skull, isolated teeth, mandible and eight associated
123 cervical and trunk vertebrae.

124 *Etymology*. Named in honour of Madam Heba Farahat Mohamed, responsible for the fossil
125 restoration in the New Valley Vertebrate Paleontology center, and who always makes great
126 efforts in preparing and restoring the vertebrate specimens.

127 *Locality*. North Gebel Gifata, Dakhla Oasis, 12 km N of Mut south Western Desert, Egypt.

128 *Horizon*. Basal part of Dakhla Shale, lower Maastrichtian, Upper Cretaceous.

129 *Diagnosis*. *Halisaurus* diagnosed by the following combination of characters: frontal long and
130 tapering anterior to orbits, with broadly convex supraorbital processes and anteriorly displaced
131 posterolateral alae. Frontal with concave midline contact with parietal. Frontal median ridge
132 developed as a sharp, narrow ridge extending the full length of the parietal. Frontal midline
133 eminence.. Parietal foramen small and subcircular. Parietal table subtriangular, with broadly
134 convex posterolateral margins. Articulation of the parietal and supratemporal obliquely oriented.
135 Quadrate conch narrow anteriorly, very broad posteriorly, and extended dorsally to quadrate
136 head. Quadrate tympanic meatus small, lenticular, and inclined. Quadrate suprastapedial process
137 broad. Large contribution of the surangular to the glenoid fossa.

138 **5. Description and Comparison**

139 **5.2 Skull**

140 The skull preserves the premaxilla, right maxilla, left jugal, frontal, parietal, left quadrate and
141 part of the braincase.

142 *Premaxilla* (Fig. 4 A-C). The premaxilla is somewhat crushed, but complete except for the
143 tapered posterior end of the bone that would have contacted the frontals. It bears four teeth. Its

144 tip is short, broad and rounded. It lacks a premental rostrum, as in *Halisaurus arambourgi* (Bardet
145 et al., 2005a), *H. platyspondylus* (Polcyn and Lamb, 2012), *Halisaurus* (“*Eonatator*”) *coellensis*
146 (Páramo-Fonseca, 2013) and *Pluridens serpentis* (Longrich et al., 2021a). Dorsally the
147 premaxilla’s tip bears several large neurovascular foramina. The narial process has a
148 subrectangular section, and is narrow anteriorly, before becoming broad posteriorly between the
149 maxillae (Fig. 4. A and B), as in *H. arambourgi*. Its antero-lateral surfaces form large and
150 regularly posteriorly curved facet for articulation with the maxillae, as in other Halosaurinae.

151 *Maxilla* (Fig. 4 D-G). The left maxilla is relatively complete, the anterior end being well-
152 preserved and the posterodorsal margin and posterior end of the bone being broken; only a
153 fragment of the right maxilla, preserving five tooth positions, is complete. The preserved part of
154 the right maxilla measures about 19 cm long. It is long, straight and low as in other Halosaurinae.
155 Though incomplete, its posterior part tapers gently to articulate with the jugal. It preserves at
156 least 10 alveoli, as well as five tooth roots, and two well-preserved crowns. The lateral surface
157 bears a row of large, slit-like foramina located above the gumline (Fig. 4 C and F). The dorsal
158 labial parapet is taller than the lingual one, such that the tooth roots are broadly exposed (Fig. 4
159 D-E), as in other Halosaurinae, and in contrast to derived mosasaurids such as Mosasaurini,
160 where the tooth roots are covered by the lingual parapet (i.e. (Bell Jr, 1997)). In medial view, the
161 interdental alveolar bone is weakly developed, as in *Halisaurus arambourgi* (Bardet et al.,
162 2005a), and in contrast with *Pluridens serpentis* and *P. walkeri* (Longrich, 2016; Longrich et al.,
163 2021a) where interdental alveolar bone is prominent.

164 *Frontal* (Figs. 5, 6). The frontal is somewhat crushed but complete, except for some minor
165 damage to the margins of the bone. The frontal is long and triangular, with a tapered anterior
166 end. At the prefrontal contact, it is wider than in *Eonatator sternbergii* and *Halisaurus*

167 *ponpetelegans* (“*Phosphorosaurus*” *ponpetelegans*, see Discussion) and more similar to
168 *Halisaurus platyspondylus*, *H. arambourgi*, and *Phosphorosaurus ortliebi* (Bardet et al., 2005a;
169 Holmes and Sues, 2000; Lingham-Soliar, 1996). The supraorbital process is elongate and
170 broadly convex, similar to *Halisaurus platyspondylus* and *H. arambourgi*. The supraorbital
171 process is much smaller in *Eonatator sternbergii* and *H. ponpetelegans*, and it has an unusual
172 rectangular shape in *Phosphorosaurus ortliebi*.

173 The frontal’s orbital margins are weakly concave, with the lateral edges of the bone being
174 almost straight. The frontals would have formed the dorsal margin of the orbits as in other
175 Halisaurini, a primitive condition. The frontal is however excluded from the orbit by a
176 prefrontal-postorbitofrontal contact in the halisaurine *Pluridens* and, convergently, in
177 Tylosaurinae and some members of Mosasaurinae (Longrich et al., 2021a) and Plioplatecarpinae
178 (Strong et al. 2020).

179 The frontal’s dorsal surface is planar in lateral view (Fig. 5C), as in *Halisaurus*
180 *platyspondylus* (Konishi et al., 2016), whereas *Eonatator sternbergii* (Bardet and Suberbiola,
181 2001) and *H. ponpetelegans* have a gently curved frontal profile (Konishi et al., 2016). A
182 prominent dorsal median ridge extends almost the entire length of the frontal (Fig. 5A). It is tall
183 anteriorly and low posteriorly, as in *H. ponpetelegans*; it is narrow and tall relative to *H.*
184 *platyspondylus*, *H. arambourgi* and *P. ortliebi*. In transverse section the median ridge is not
185 constricted at its base as in *H. ponpetelegans* but is broad, making a triangular ridge, with a
186 narrow tip and wide base. The ridge gradually expands to form a triangular eminence near the
187 posterior margin.

188 This triangular median eminence or median boss is a derived feature of Halisaurini, but is
189 absent in *Pluridens* (Longrich et al., 2021a). The triangular eminence in *H. hebae* is low but well

190 defined, relatively long, and bounded posteriorly by two ridges. The triangular eminence extends
191 between the orbits, as in *H. arambourgi*, *H. ponpetelegans* and *Phosphorosaurus ortliebi*; that of
192 *H. platyspondylus* is short (Fig. 6). The triangular eminence is also relatively narrow, unlike the
193 broad eminence in *H. arambourgi* and *H. platyspondylus* (Bardet et al., 2005a).

194 The frontal's posterior margin has an undulating shape (Fig. 6). The posterolateral alae are
195 slightly displaced anteriorly, as in *Halisaurus platyspondylus* and *H. arambourgi*; they are
196 posteriorly positioned in *Eonatator sternbergii*, *Halisaurus ponpetelegans*, and *Phosphorosaurus*
197 *ortliebi*. The median frontoparietal contact is concave, similar to *Eonatator sternbergii*, *H.*
198 *ponpetelegans*, and *H. platyspondylus*; that of *H. arambourgi* is convex.

199 The frontal's ventral surface (Fig. 5B) bears two prominent, parallel ridges bounding a long
200 and elliptical median groove for the olfactory stalks (Bardet et al., 2005a). Oval facets for
201 articulation with the prefrontal lie lateral to these ridges. The facets for articulation with the
202 postorbitofrontal are not distinct.

203 *Parietal* (Fig. 7). The parietal, is incomplete, with its anterolateral ends and one of the
204 posterolateral rami broken away, but relatively three-dimensional. It is a large and robust
205 element, measuring in its current state of preservation, two thirds of the frontal length. In dorsal
206 view, the parietal table is roughly triangular and smooth, resembling that of *H. platyspondylus*
207 (Holmes and Sues, 2000); it is very different from that of *H. arambourgi* whose median surface
208 is elongated, sub-rectangular in shape with convex lateral edges and ornamented by numerous
209 transversal undulated ridges (Bardet et al., 2005a; Polcyn et al., 2012). The parietal foramen is
210 circular and small relative to the parietal, unlike *Halisaurus platyspondylus*, *H. arambourgi*
211 (Bardet et al., 2005a; Holmes and Sues, 2000) and *H. ponpetelegans* (Konishi et al., 2016)), and
212 much smaller than in *Phosphorosaurus ortliebi* (Lingham-Soliar, 1996). It lies anteriorly on the

213 parietal table, without crossing the suture with frontal like in *P. ortliebi*, and is slightly raised
214 relative to the dorsal surface of the parietal table, but without a surrounding ridge like in *H.*
215 *arambourgi*. In ventral view, a pair of depressions lies on either side of the parietal foramen, as
216 in other Halisaurini. As in *H. arambourgi*, the foramen opens ventrally on a triangular eminence
217 (Fig. 7B), forming a sulcus between it and the descending process on either side. The foramen
218 passes obliquely through the parietal, so its ventral opening is located more posteriorly than the
219 dorsal one.

220 The left suspensorial ramus, though incomplete, is broad and dorsoventrally compressed
221 unlike in *H. arambourgi* where it is mediolaterally compressed (Bardet et al., 2005a); it gently
222 slopes ventrally to articulate with the supratemporal. The supratemporal articulation facet is not
223 vertically oriented as in *H. ponpetelegans* and *H. platyspondylus*, but faces slightly oblique
224 ventrolaterally like in *H. arambourgi*.

225 *Jugal* (Fig. 8). The jugal generally resembles that of *H. arambourgi* and *H. ponpetelegans*,
226 having a broadly arched shape. However, its ascending ramus is relatively broader than in these
227 two taxa (Bardet et al., 2005a; Konishi et al., 2016). The horizontal ramus and the ascending
228 ramus are equal in size. The horizontal ramus is much more slender than the ascending one. . The
229 posteroventral process is lacking, like in *H. arambourgi*. The angle between the horizontal and
230 the ascending rami is more than 120 degrees, like in *H. arambourgi* (Bardet et al., 2005a). The
231 large and broadly arched jugal is associated with an increase in orbit size in the Halisaurini (e.g.
232 Konishi et al., 2016).

233 *Quadrate* (Fig. 9). The left quadrate is three dimensional and relatively well-preserved
234 except for the posterodorsal margin of the lateral conch, which has been damaged. It resembles

235 that of *H. arambourgi* but is slightly more robust (Fig. 9). It has a typical question-mark shape in
236 lateral view.

237 The suprastapedial process is large and broad, relatively wider than in *H. arambourgi* and *H.*
238 *platyspondylus*. As in these species, it is greatly inflated distally (Fig. 9B, D). A distinct U-
239 shaped shallow depression lies on the posterior distal face of the suprastapedial process, dividing
240 it into two parts (Fig. 9B), like in *H. arambourgi* (Bardet et al., 2005a). The infrastapedial
241 process is also well developed, forming a very large oblique process (Fig. 9B, D). As in others
242 halisaurines, the infrastapedial process is coalescent but not fused to the suprastapedial process.

243 The tympanic meatus (or stapedial notch) is small, lenticular, located on the upper part of the
244 quadrate shaft and obliquely oriented (Figs. 9C-D). These characters differ from *H.*
245 *platyspondylus* and *H. arambourgi*, which have a relatively large, teardrop-shaped vertical
246 tympanic meatus, and from *H. ponpetelegans* and *P. ortliebi* which have a very large (compared
247 to the quadrate height) vertical and slender elliptical shaped tympanic meatus.

248 In medial view (Fig. 9D), the quadrate has a curved median ridge that lies parallel to the
249 tympanic meatus. A similar ridge is also seen in *H. ponpetelegans*, *P. ortliebi* and *H. arambourgi*
250 (Bardet et al., 2005a; Konishi et al., 2016; Lingham-Soliar, 1996) whereas it is vertical in *H.*
251 *platyspondylus* (Holmes and Sues, 2000). The stapedial pit is small, narrow, and oval, located
252 anteriorly, near the dorsal margin of the stapedial notch. It is inclined posterodorsally as in *H.*
253 *platyspondylus*, *H. arambourgi*; in *H. ponpetelegans* it is vertical.

254 In lateral view (Fig. 9C), the anterior tympanic ala extends as a thin steep arch from the
255 suprastapedial process to the condyle. The quadrate conch is relatively narrow anteriorly to the
256 tympanic meatus, then expands both posteriorly and dorsally. The quadrate conch resembles in
257 its general shape that of *H. arambourgi* and is distinct from that of *H. ponpetelegans* and

258 especially *H. platyspondylus* where the conch is strongly expanded anteriorly (Holmes and Sues,
259 2000). The dorsal extension of the quadrate conch is shared with *H. platyspondylus* and *H.*
260 *arambourgi*.

261 The distal condyle has a robust, crescentic shape; it is laterally convex and medially planar
262 (Fig. 9F). It resembles that of *H. platyspondylus* and *H. ponpetelegans* but differs from *H.*
263 *arambourgi* which is convex from side to side. As in all halisaurines, it is orientated
264 perpendicular to the proximal head (Fig. 9E). The basin-like alar concavity located directly
265 above the mandibular condyle is large (Fig. 9E) as in *H. platyspondylus* and *H. ponpetelegans*.

266 *Braincase* (Fig. 10). The braincase is relatively complete and three-dimensional. As is usual
267 in mosasaurids, it is composed of several tightly sutured bones. It preserves parts of the
268 basioccipital, basisphenoid, prootic, opisthotic-exoccipital, supraoccipital and supratemporal. As
269 bones are difficult to differentiate due to poor preservation, the braincase complex is described as
270 a whole, rather than bone by bone.

271 In ventral view (Fig. 10A), the main part of the braincase is occupied by the central
272 basioccipital and a small part of the basisphenoid. The basioccipital is robust and square, as usual
273 in mosasaurids (i.e.(Russell, 1967)). The basioccipital condyle and the basal tubera are poorly
274 preserved and separated by a groove. The basal tubera (sphenoccipital tubercles) are thick, taller
275 than wide, and the paired basal tubera diverge posteriorly to form a triangular shape; they are
276 separated one from each other by a hollow between the basal tubera. The anterior suture with the
277 basisphenoid is transverse. Only the posteriormost part of this bone is preserved. The prootic and
278 paraoccipital process of the opisthotic-exoccipital are tightly sutured; they are posterolaterally
279 oriented and articulate with the supratemporal.

280 In dorsal view (Fig. 10B) the same configuration is seen. The basioccipital bears a deep
281 median groove corresponding to the floor of the medullar canal. Laterally, on its left side are two
282 ascending laminae of bone that constitute the lateral wall of the medullar cavity; the anterior is
283 the only preserved part of the prootic, whereas the posterior one corresponds to the basal part of
284 the opisthotic-exoccipital paroccipital process. A transverse suture between them is visible on
285 both sides. The transverse suture between the basal tubera of the basioccipital and the abutting
286 posterior ala of the basisphenoid is still visible on the left side. The supraoccipital roofs the
287 posterior part of the medullar cavity and articulates laterally with the paroccipital process of the
288 opisthotic-exoccipital.

289 **5.3 Mandible**

290 Most elements of the left mandible are preserved, including the dentary, splenial, coronoid,
291 angular and fused surangular-articular. They broadly resemble other *Halisaurus* (Fig. 11).

292 *Dentary* (Fig. 11A-B). Most of the left dentary is preserved, except for the anterior tip and the
293 bone's ventral margin. It measures ~20 cm in length. Tooth count cannot be determined, but
294 there were at least 15 alveolae, similar to the condition in other halisaurines but fewer than the 25
295 or more found in *Pluridens*. As in the maxilla, the dorsal labial parapet is taller than the lingual
296 one, such that the dental alveolae are visible in lingual view (Fig. 11B), as in other Halisaurinae.
297 The dentary's dorsal and ventral margins are straight (Fig. 11A-B). The dentary's lateral surface
298 is gently convex, and bears a dorsal row of elongated, slit-like foramina marking the exit of the
299 terminal branches of the 5th mandibular nerve (Russell, 1967). The dentary's medial surface is
300 concave, with a deep Meckelian canal (Bardet et al., 2005a) beginning near the anterior tip of the
301 bone and widening posteriorly to form the mandibular channel.

302 *Splénial (Fig. 11C-D)*. The left splénial is well-preserved except for the dorsal margin, which
303 is broken away. It has an elongated wedge shape with lateral and medial wings, the medial one,
304 generally higher and very thin, being partially broken. The lateral wing is straight, without any
305 posterior curvature (Fig. 11F), in contrast with *H. ponpetelegans*. A large foramen for the
306 inferior alveolar nerve lies on the medioventral surface of the medial wing, in front of the
307 splénial cotyle, whose articulation is tear-drop shaped.

308 *Angular (Fig. 11G)*. The angular is relatively well-preserved. It is a laterally compressed
309 cone with a wide, thick, curved base tapering posteriorly. The posterior part of the bone tapers
310 ventral to the surangular (Fig. 11.G). The condyle for the splénial articulation is convex.

311 *Coronoid (Fig. 11E-F)*. The coronoid is largely complete except for the anterior tip of the
312 bone and some damage to the posteroventral margin. It generally resembles *H. arambourgi*
313 (Bardet et al., 2005a) and *H. ponpetelegans* (Konishi et al., 2016). It has a long, narrow arched
314 shape and sits like a saddle on the surangular's dorsal surface. The lateral and medial descending
315 wings are poorly developed and most probably did not cover the pre-articular process of the
316 articular medially. The posterior ascending process is large as in other halisaurines, including
317 *Halisaurus* and *Pluridens* (Longrich et al. 2021); the ascending process is proportionally smaller
318 and lower in plioplatecarpines and tylosaurines (Russell, 1967).

319 *Surangular – Articular (Fig. 11H-J)*. The surangular – articular is relatively complete and
320 three-dimensional. The bones are tightly and measure 24 cm. It is a long and narrow rectangular
321 complex resembling that of other Halisaurinae. The complex is gently convex laterally and
322 concave medially.

323 In lateral or medial view, the surangular bears a long, horizontal margin between the glenoid
324 cavity and the coronoid zone, articulation, which is long and gently concave. The surangular's
325 ventral margin is straight. The suture with the articular is gently curved.

326 In medial view, the surangular is covered by the long, straight prearticular process of the
327 articular. Dorsal to its posterior part, the adductor fossa is large and concave. The coronoid
328 articulation is long and slender, sloping from the posterior process to the anterior end of the
329 bone. The retroarticular process is round and vertically oriented as in *H. platyspondylus*, *H.*
330 *arambourgi* and *Eonatator sternbergii* (Bardet et al., 2005a; Holmes and Sues, 2000). The
331 glenoid fossa is deep and bears a large anterior 'lip' as in other Halisaurinae. The contribution of
332 the surangular to the glenoid fossa - about 2/3, versus 1/3 by the articular - is large compared
333 with other halisaurines.

334 **5.4 Dentition**

335 Two well-preserved teeth are ankylosed to the maxilla. Several broken teeth tooth bases are
336 ankylosed to the dentary, and several teeth were found isolated (Figs 3, 4, 12). Tooth crowns are
337 small, approximately 14 mm tall. They have a sharply pointed apex. The crown rises vertically or
338 slopes slightly anteriorly, and then is abruptly posteriorly curved at the midpoint of the crown.
339 This strong hooking of the teeth is typical of Halisaurinae (Bardet et al., 2005a) and some
340 Plioplatecarpinae such as *Plioplatecarpus*. The enamel is very finely striated, as is typical of
341 Halisaurinae (Bardet et al., 2005a; Longrich, 2016) and bears weak, unserrated, anterior and
342 posterior carinae; the anterior carina is relatively stronger than the posterior one. The crown's
343 basal cross-section is circular, with lingual and buccal surfaces being equally convex. The base
344 of the root lacks fluting. Teeth bear deep replacement pits which lie on the medial surface of the
345 tooth base, as in other halisaurines.

346 **5.5 Postcranial skeleton**

347 Four cervical vertebrae and four dorsal vertebrae, found associated with the skull and
348 mandible remains, are present in various degrees of preservation (Fig. 13). The vertebrae are
349 highly deformed, being compressed by overburden shales, but many features can be recognized.
350 In all vertebrae, the zygosphene–zygantrum complex is absent as in other halisaurines (Bardet et
351 al., 2005a), and prezygapophyses and postzygapophyses are large.

352 The axis vertebra (Fig. 13A-B) is well preserved, with a long, narrow centrum. The neural
353 spine is long and broad, as usual for halisaurines. Synapophyses are small, dorsoventrally
354 compressed, and project from the posterior third of the centrum. The hypapophysis is large,
355 robust, lies posteriorly on the centrum's ventral surface and is obliquely oriented in lateral view.
356 It is connected anteriorly by a narrow longitudinal ridge to the ventral rim of the articular facet
357 for the axial intercentrum, as in *H. ponpetelegans* (Konishi et al., 2016). The condyle articulation
358 has a roughly triangular shape in posterior view. The cotyle is partially broken. The neural canal
359 is triangular in shape and taller than wide. Postzygapophyses are large and dorsolaterally
360 inclined.

361 The other three cervical vertebrae (Fig. 13 C-E) have small, narrow hypapophyses, indicating
362 that they come from the posterior part of the cervical series, and more dorsoventrally compressed
363 sub-rectangular condyle and cotyle articulations (height: width ratio = 1: 2) as in others
364 Halisaurinae (i.e. (Bardet et al., 2005a; Bell Jr, 1997; Russell, 1967)). The synapophyses are
365 wide, robust and have a wing-like appearance. They extend ventrally to the ventral surface of the
366 centrum, a halisaurine characteristic (Bardet et al., 2005a). Dorsally, the synapophyses are
367 connected to the prezygapophyses by a descending crest. The postzygapophyses extend

368 mediolaterally from the neural arch. The neural canal is oval-shaped and wider than tall. The
369 neural spines of the three vertebrae are partially broken.

370 The trunk vertebrae (Fig. 13 F-G) are much larger than the cervicals, and their centra are
371 dorsoventrally compressed, as in halisaurines (Polcyn et al., 2012). The synapophyses are located
372 anteriorly and connect to the cotyle. The neural spine is tall and anteroposteriorly wide, almost
373 vertical. The neural canal is oval shaped, and is wider than tall. Postzygapophyses remain robust.

374 6. Discussion

375 *Affinities of Halisaurus hebae nov. sp. and systematics of Halisaurinae*

376 *Halisaurus hebae* can be referred to Halisaurinae based on a combination of primitive and
377 derived characters. The parietal has an oblique contact with the supratemporal (Bardet et al.,
378 2005). The quadrate has a large infrastapedial process contacting the suprastapedial process. The
379 zygosphene–zygantrum complex is absent; synapophyses of the cervical vertebrae extend
380 dorsoventrally to the ventral surface of the centrum (Bardet et al., 2005a). Teeth are small and
381 conical, with their apices pointed and hooked posteriorly as in other *Halisaurus* species and
382 *Pluridens* (Bardet et al., 2005a; Longrich et al., 2021a).

383 Among Halisaurinae, NVP030 shares characters with Halisaurini, and specifically species of
384 *Halisaurus* Marsh, 1869. The frontal resembles Halisaurini in participating in the orbit margins,
385 in having a prominent dorsal median keel extending almost its full length and terminating
386 posteriorly in a triangular boss (Bardet et al., 2005a), and in having a ventral boss articulating
387 with the parietal. The parietal is typical of Halisaurini in having depressions on the parietal table
388 lateral to the parietal foramen. The very large, slender, and comma-shaped jugal also

389 characterizes Halisaurini (Longrich et al., 2021a). The condyles and cotyles of cervical vertebrae
390 are subrectangular (Russell, 1967).

391 The anterior expansion of the frontal between the prefrontals seen in *H. hebae* is shared with
392 *H. platyspondylus*, and *H. arambourgi*, suggesting affinities with this clade. The anterior
393 displacement of the frontal posterolateral alae is absent in *Eonatator sternbergii* and *H.*
394 *ponpetelegans*, but again is shared with *H. platyspondylus* and *H. arambourgi*. Likewise, the
395 oblique orientation of the suspensorial ramus is shared with *H. platyspondylus* and *H.*
396 *arambourgi* whereas they are vertical in *H. ponpetelegans*. This suggests that *H. hebae*
397 represents the sister-taxon to the *H. platyspondylus*-*H. arambourgi* clade.

398 NVP030 can be distinguished from the related *H. platyspondylus*-*H. arambourgi* clade by
399 the more elongate and tapered anterior end of the frontal. The parietal also has a smaller parietal
400 foramen, and is less elongate posteriorly. The quadrate tympanic meatus is smaller, more
401 lenticular, and has an oblique orientation; *H. platyspondylus* and *H. arambourgi* have a relatively
402 larger, inverse teardrop outline of the meatus. The surangular is much elongated and low, its
403 contribution to the glenoid fossa is large when compared with other *Halisaurus*,
404 *Phosphorosaurus* and *Eonatator* species.

405 We conducted a phylogenetic analysis of the Halisaurinae building on the previous analysis
406 by Longrich et al. (2021). The analysis includes 31 characters and 11 ingroup taxa. Phylogenetic
407 analysis recovers 3 most parsimonious trees (Consistency Index = 0.6604, Retention Index =
408 0.7568) (Fig. 14).

409 The phylogeny presented here is inconsistent with some previous classifications of
410 Halisaurinae (Konishi et al., 2016; Páramo-Fonseca, 2013). We did not find character support

411 for a sister-taxon relationship between *Phosphorosaurus ortliebi* and *Halisaurus ponpetelegans*
412 (“*Phosphorosaurus*” *ponpetelegans*), and could not repeat this result with the current, and more
413 comprehensive analysis. We suggest that this species be provisionally removed to *Halisaurus*, as
414 *Halisaurus ponpetelegans*, but it may be appropriate to designate a distinct genus, given that it
415 appears to be distinct from other *Halisaurus*.

416 Similarly, we found no support for a sister-taxon relationship between *Eonatator sternbergii*
417 and *Halisaurus coellensis* (“*Eonatator*” *coellensis*). Instead *H. coellensis* clusters with
418 Maastrichtian *Halisaurus* spp., consistent with its stratigraphic position high in the Campanian.
419 We provisionally assign this species to *Halisaurus* pending further revision. Additional study
420 and more fossils are needed to revise halisaurine taxonomy, but the Halisaurinae appear to be far
421 more diverse than previously thought, complicating their taxonomy.

422 *Halisaurine biology*

423 *Halisaurus hebae* has a large, broadly curved jugal which would have extended below the
424 maxilla. This large bowed jugal is absent in *Phosphorosaurus ortliebi* and *Pluridens serpentis*,
425 but is shared with other *Halisaurus*, including *H. ponpetelegans*, *H. coellensis*, and *H.*
426 *arambourgi*. Although the postorbitofrontal is not known for all taxa, *H. ponpetelegans* and *H.*
427 *coellensis* show that *Halisaurus* spp. had a long, posteroventrally extended jugal process of the
428 postorbitofrontal, that is absent in *P. ortliebi* and *P. serpentis*. These adaptations suggest the
429 large, anterolaterally orbits described for *H. ponpetelegans* are characteristic of *Halisaurus* as a
430 whole.

431 The large, anterolaterally directed orbits of *Halisaurus* suggest it relied heavily on vision for
432 foraging, in contrast to *Pluridens*, where the orbits are reduced (Longrich et al., 2021a). The low

433 number of neurovascular foramina in the premaxilla, which are elaborated in *Pluridens*, likewise
434 suggests a shift from tactile foraging towards visual foraging.

435 The functional significance of this adaptation is unclear. Large eyes occur in several marine
436 reptiles taxa such ichthyosaurs and were probably used for vision in obscure deep ocean
437 environments (i.e. Motani et al., 1999; Yamashita et al., 2015). They are also occur in nocturnal
438 birds such as owls and nightjars (Brooke et al., 1999; Hall and Ross, 2007), with large eyes
439 serving to increase eyes sensitivity to light in low-light environments. However, large eyes also
440 occur in diurnal birds such as hawks and falcons (Brooke et al., 1999) to increase the eye's
441 resolution (Mitkus et al., 2018). Nocturnal adaptation is also a function not just of eye size but
442 eye shape, with nocturnal birds tending to have larger eye diameters relative to length (Hall and
443 Ross, 2007). In the absence of well-preserved sclerotic rings, it is difficult to constrain the eye
444 shape of *Halisaurus*. Binocular vision is similarly seen in both nocturnal birds, such as nightjars
445 and owls, and diurnal birds like hawks, eagles, and falcons.

446 Among modern marine mammals, large eyes and binocular vision are seen in seals, with
447 extreme orbital enlargement and binocular vision seen in the Baikal Seal, *Pusa sibirica* (Endo et
448 al., 1999). Baikal Seals engage in nocturnal foraging, but also forage during the day, when they
449 dive to greater depths (Watanabe et al., 2004). Among marine reptiles, large eyes are seen in
450 ichthyosaurs, and are thought to be an adaptation for the low light conditions encountered in
451 deep diving (Motani et al., 1999). Studies of paleopathology suggest that *Halisaurus* rarely
452 suffered from the avascular necrosis of bone tissue common to deep-divers, however (Rothschild
453 and Martin, 2005). This suggests that the large eyes of halisaurines may represent an adaptation
454 for nocturnal foraging, as previously proposed (Konishi et al., 2016), rather than deep diving.

455 While the function of these large eyes remains uncertain, they show how mosasaurids had
456 diverse foraging strategies in the latest Cretaceous, paralleling the diversification of tooth and
457 jaw morphologies (Bardet et al., 2015) and locomotor strategies (Lingham-Soliar, 1992).
458 Towards the end of the Cretaceous, mosasaurids were highly diverse in how they sensed their
459 environment, how they moved through their environment, and their diets.

460 *Implications for mosasaur biodiversity and biogeography*

461 Early discoveries of mosasaurids were primarily made in relatively high-latitude regions of
462 Europe e.g. (Bardet and Pereda-Suberbiola, 1996; Jagt et al., 2006; Lingham-Soliar, 1998;
463 Lingham-Soliar and Nolf, 1989; Schulp et al., 2006) and North America (Bell Jr, 1997; Russell,
464 1967). Later work has revealed a diverse mosasaurid fauna in the subtropics of Africa and the
465 Middle East, with a plethora of taxa now known from Israel (Bardet, 2012; Christiansen and
466 Bonde, 2002), Jordan (Bardet and Pereda Suberbiola, 2002; Kaddumi, 2009), Syria (Bardet et al.,
467 2000), Egypt (Bardet, 2012; Zdansky, 1934), Morocco (Bardet et al., 2015; Bardet et al., 2005a;
468 Bardet et al., 2008; Bardet et al., 2005b; Bardet et al., 2004; LeBlanc et al., 2012; Longrich et al.,
469 2021a; Longrich et al., 2021b; Longrich et al., 2022; Polcyn et al., 2012; Rempert et al., 2022;
470 Schulp et al., 2009; Strong et al., 2020), Niger and Nigeria (Lingham-Soliar, 1991, 1998;
471 Longrich, 2016) and Angola (Schulp et al., 2008).

472 Although halisaurines are rare and low in diversity in higher-latitude settings, they are a
473 common, diverse component of subtropical assemblages (Longrich et al., 2021a). The discovery
474 of a new taxon from Egypt adds to the diversity of halisaurines from the Tethyan realm, and
475 emphasizes the endemism of mosasaurids. As large, pelagic animals, mosasaurids should be able
476 to disperse long distances, but distinct species and faunal compositions occur in different parts of
477 the world. Precisely why, remains unknown. Mosasaurids may have had elevated metabolic rates

478 compared to other lizards, with a degree of endothermy (Bernard et al., 2010; Harrell Jr et al.,
479 2016) But this may have varied within Mosasauridae, with some being better able to regulate
480 their temperatures in cooler waters, and others more cold-intolerant. Mosasaurs also show
481 remarkable variation in tooth and jaw morphology, showing dietary specialization. To the extent
482 that prey showed regional differences, predators would have as well.

483 These patterns complicate attempts to understand global changes in mosasaur diversity.
484 Polcyn et al. (2014) suggested that halisaurines declined in the Maastrichtian, but their
485 abundance and diversity in the Maastrichtian of the subtropics suggests that this is an artifact of
486 sampling and study that have tended to favor more temperate environments. On the contrary,
487 halisaurines seem to stage a radiation paralleling that of the Mosasaurinae (Polcyn et al., 2014) in
488 the latest Cretaceous (Fig. 14). Similarly, Tylosaurinae seem to be rare in lower-latitude
489 environments, but seem to remain important parts of the fauna in high-latitude environments
490 (Jiménez-Huidobro and Caldwell, 2016; Novas et al., 2002). Marine reptiles show different
491 diversity patterns in different parts of the world.

492 7. Conclusions

493 Fossils from the lower Maastrichtian of the Dakhla Shale of Egypt, Dakhla Oasis, document
494 a new species of *Halisaurus*. The new species, *Halisaurus hebae*, shows close affinities with the
495 upper Maastrichtian *Halisaurus arambourgi* from Morocco and *H. platyspondylus* from the East
496 Coast of the United States. Halisaurines were diverse and important in marine ecosystems during
497 the Maastrichtian, staging a major radiation alongside the larger Mosasaurinae in the latest
498 Cretaceous, with Halisaurini likely specializing in nocturnal foraging. Halisaurines may have
499 been more diverse and common in lower-latitude environments, especially the Tethys and
500 eastern Atlantic.

501

502 **Acknowledgements.** The authors sincerely thank New Valley University for funding the
503 field trips as well as the laboratory preparation of the specimens. Additionally, the authors would
504 like to thank Dr. Nabil Hanafi, the Head of Mut city for his hospitality and great support during
505 the field trips. Great thanks are extended to Mr. Essam Yousef New Valley University, for his
506 great efforts in collecting fossils.

References

- 507 AbdelGawad, M.K., El-Kheir, G.A.A., Kassab, W.G., 2021. The youngest records of mosasaurid reptiles
508 from the Upper Cretaceous of the South-Western Desert in Egypt. *Proceedings of the Geologists'*
509 *Association* 132, 556-562.
- 510 Abu El-Kheir, G.-M., Abdelgawad, M.K., Kassab, W.G., 2021. First known gigantic sea turtle from the
511 Maastrichtian deposits in Egypt. *Acta Palaeontologica Polonica* 66.
- 512 Abu El-Kheir, G.A., Tantawy, A.A., Mousa, M.K., Wahba, D.G.A., Capasso, L., 2022. *Diastemapycnodus*
513 *Tavernensis* Gen. et Sp. Nov.(Actinopterygii,† Pycnodontiformes) from the Marine Maastrichtian (Late
514 Cretaceous) of the Dakhla Formation, Western Desert, Egypt. *Historical Biology* 34, 2324-2331.
- 515 Bardet, N., 2012. Maastrichtian marine reptiles of the Mediterranean Tethys: a palaeobiogeographical
516 approach. *Bulletin de la Société Géologique de France* 183, 573-596.
- 517 Bardet, N., Cappetta, H., Suberbiola, X.P., Mouty, M., Al Maleh, A., Ahmad, A., Khrata, O., Gannoum, N.,
518 2000. The marine vertebrate faunas from the Late Cretaceous phosphates of Syria. *Geological Magazine*
519 137, 269-290.
- 520 Bardet, N., Houssaye, A., Vincent, P., Suberbiola, X.P., Amaghaz, M., Jourani, E., Meslouh, S., 2015.
521 Mosasaurids (Squamata) from the Maastrichtian phosphates of Morocco: biodiversity,
522 palaeobiogeography and palaeoecology based on tooth morphoguilds. *Gondwana Research* 27, 1068-
523 1078.
- 524 Bardet, N., Pereda-Suberbiola, X., 1996. Las faunas de reptiles marinos del Cretácico final de Europa
525 (margen norte del Tetis mediterráneo). *Spanish Journal of Palaeontology* 11, 91-99.
- 526 Bardet, N., Pereda Suberbiola, X., 2002. Marine reptiles from the Late Cretaceous Phosphates of Jordan:
527 palaeobiogeographical implications. *Geodiversitas* 24, 831-839.
- 528 Bardet, N., Pereda Suberbiola, X., Iarochene, M., Bouya, B., Amaghaz, M., 2005a. A new species of
529 *Halisaurus*. from the Late Cretaceous phosphates of Morocco, and the phylogenetical relationships of
530 the Halisaurinae (Squamata: Mosasauridae). *Zoological Journal of the Linnean Society* 143, 447-472.
- 531 Bardet, N., Pereda Suberbiola, X., Schulp, A.S., Bouya, B., 2008. New material of *Carinodens* (squamata,
532 mosasauridae) from the Maastrichtian (late cretaceous) phosphates of Morocco, *Proceedings of the*
533 *Second Mosasaur Meeting*. Fort Hays Studies, Special, pp. 29-36.
- 534 Bardet, N., Suberbiola, X.P., 2001. The basal mosasaurid *Halisaurus sternbergii* from the Late Cretaceous
535 of Kansas (North America): a review of the Uppsala type specimen. *Comptes Rendus de l'Académie des*
536 *Sciences-Series IIA-Earth and Planetary Science* 332, 395-402.
- 537 Bardet, N., Suberbiola, X.P., Iarochène, M., Amalik, M., Bouya, B., 2005b. Durophagous Mosasauridae
538 (Squamata) from the Upper Cretaceous phosphates of Morocco, with description of a new species of
539 *Globidens*. *Netherlands Journal of Geosciences* 84, 167-175.
- 540 Bardet, N., Suberbiola, X.P., Iarochene, M., Bouyahyaoui, F., Bouya, B., Amaghaz, M., 2004. *Mosasaurus*
541 *beaugei* Arambourg, 1952 (Squamata, Mosasauridae) from the late Cretaceous phosphates of Morocco.
542 *Geobios* 37, 315-324.
- 543 Bell Jr, G.L., 1997. A phylogenetic revision of North American and Adriatic Mosasauroida, Ancient
544 marine reptiles. Elsevier, pp. 293-332.
- 545 Bernard, A., Lécuyer, C., Vincent, P., Amiot, R., Bardet, N., Buffetaut, E., Cuny, G., Fourel, F., Martineau,
546 F., Mazin, J.-M., 2010. Regulation of body temperature by some Mesozoic marine reptiles. *Science* 328,
547 1379-1382.
- 548 Brooke, M.d.L., Hanley, S., Laughlin, S., 1999. The scaling of eye size with body mass in birds.
549 *Proceedings of the Royal Society of London. Series B: Biological Sciences* 266, 405-412.

550 Caldwell, M.W., Bell Jr, G.L., 1995. *Halisaurus* sp.(Mosasauridae) from the Upper Cretaceous (?
551 Santonian) of east-central Peru, and the taxonomic utility of mosasaur cervical vertebrae. Journal of
552 Vertebrate Paleontology 15, 532-544.

553 Capasso, L., Abdel Aziz, T., Mohamed Kamel, M., Gamal Ahmed, W.D., Gebely Abdelmaksoud, A.E.-K.,
554 2021. *Anomoeodus aegypticus* n. sp.(Pisces,† Pycnodontiformes) from the late Cretaceous of the Dakhla
555 Formation, Western Desert, Egypt. Thalassia Salentina 43, 89-104.

556 Christiansen, P., Bonde, N., 2002. A new species of gigantic mosasaur from the Late Cretaceous of Israel.
557 Journal of Vertebrate Paleontology 22, 629-644.

558 Dollo, L., 1889. Note sur les vertébrés récemment offerts au Musée de Bruxelles par M. Alfred
559 Lemonnier. Bulletin de la Société belge de Géologie, de Paléontologie et d'Hydrologie 3, 181-182.

560 Endo, H., Sasaki, H., Hayashi, Y., Petrov, E.A., Amano, M., Suzuki, N., Miyazaki, N., 1999. CT examination
561 of the head of the Baikal seal (*Phoca sibirica*). The Journal of Anatomy 194, 119-126.

562 Gervais, P., 1853. Observations relatives aux reptiles fossiles de France. Comptes Rendus hebdomadaires
563 des séances de l'Académie des Sciences 36, 470.

564 Hall, M., Ross, C., 2007. Eye shape and activity pattern in birds. Journal of Zoology 271, 437-444.

565 Harrell Jr, T.L., Pérez-Huerta, A., Suarez, C.A., 2016. Endothermic mosasaurs? Possible thermoregulation
566 of Late Cretaceous mosasaurs (Reptilia, Squamata) indicated by stable oxygen isotopes in fossil
567 bioapatite in comparison with coeval marine fish and pelagic seabirds. Palaeontology 59, 351-363.

568 Hewaidy, A.G.A., Farouk, S., Bazeen, Y.S., 2017. Sequence stratigraphy of the maastrichtian-paleocene
569 succession at the dakhla oasis, western desert, Egypt. Journal of African Earth Sciences 136, 22-43.

570 Holmes, R.B., Sues, H.-D., 2000. A partial skeleton of the basal mosasaur *Halisaurus platyspondylus* from
571 the Severn Formation (Upper Cretaceous: Maastrichtian) of Maryland. Journal of Paleontology 74, 309-
572 316.

573 Jagt, J.W., Motchurova-Dekova, N., Cappetta, H., Schulp, A.S., 2006. Latest Cretaceous mosasaurs and
574 lamniform sharks from Labirinta cave, Vratsa district (northwest Bulgaria): a preliminary note. Geološki
575 anali Balkanskoga poluostrva 67, 51-63.

576 Jiménez-Huidobro, P., Caldwell, M.W., 2016. Reassessment and reassignment of the early Maastrichtian
577 mosasaur *Hainosaurus bernardi* Dollo, 1885, to Tylosaurus Marsh, 1872. Journal of Vertebrate
578 Paleontology 36, e1096275.

579 Kaddumi, H.F., 2009. Fossils of the Harrana Fauna and the adjacent areas. Eternal River Museum of
580 Natural History The Hashemite Kingdom of Jordan.

581 Konishi, T., Caldwell, M.W., Nishimura, T., Sakurai, K., Tanoue, K., 2016. A new halisaurine mosasaur
582 (Squamata: Halisaurinae) from Japan: the first record in the western Pacific realm and the first
583 documented insights into binocular vision in mosasaurs. Journal of Systematic Palaeontology 14, 809-
584 839.

585 LeBlanc, A., Caldwell, M., Bardet, N., 2012. A new mosasaurine from the Maastrichtian (U. Cretaceous)
586 phosphates of Morocco and the implications for the systematics of the Mosasaurinae. Journal of
587 Vertebrate Paleontology 32, 1-23.

588 Lindgren, J., Siverson, M., 2005. *Halisaurus sternbergi*, a small mosasaur with an intercontinental
589 distribution. Journal of Paleontology 79, 763-773.

590 Lingham-Soliar, T., 1991. Mosasaurs from the upper Cretaceous of Niger. Palaeontology 34, 653-670.

591 Lingham-Soliar, T., 1992. The tylosaurine mosasaurs (Reptilia, Mosasauridae) from the upper Cretaceous
592 of Europe and Africa. Bulletin de l'Institut Royal des Sciences naturelles de Belgique, Sciences de la Terre
593 62, 171-194.

594 Lingham-Soliar, T., 1996. The first description of *Halisaurus* (Reptilia Mosasauridae) from Europe, from
595 the Upper Cretaceous of Belgium. Bulletin de l'Institut Royal des Sciences Naturelles de Belgique,
596 Sciences de la Terre 66, 129-136.

597 Lingham-Soliar, T., 1998. A new mosasaur *Pluridens walkeri* from the Upper Cretaceous, Maastrichtian
598 of the Iullemeden Basin, southwest Niger. *Journal of Vertebrate Paleontology* 18, 709-717.

599 Lingham-Soliar, T., Nolf, D., 1989. The mosasaur *Prognathodon* (Reptilia, Mosasauridae) from the Upper
600 Cretaceous of Belgium. *Bulletin van het Koninklijk Belgisch Instituut voor Natuurwetenschappen.*
601 *Aardwetenschappen= Bulletin de l'Institut Royal des Sciences Naturelles de Belgique. Sciences de la*
602 *Terre.*

603 Longrich, N.R., 2016. A new species of *Pluridens* (Mosasauridae: Halisaurinae) from the upper
604 Campanian of Southern Nigeria. *Cretaceous Research* 64, 36-44.

605 Longrich, N.R., Bardet, N., Khaldoune, F., Yazami, O.K., Jalil, N.-E., 2021a. *Pluridens serpentis*, a new
606 mosasaurid (Mosasauridae: Halisaurinae) from the Maastrichtian of Morocco and implications for
607 mosasaur diversity. *Cretaceous Research* 126, 104882.

608 Longrich, N.R., Bardet, N., Schulp, A.S., Jalil, N.-E., 2021b. *Xenodens calminechari* gen. et sp. nov., a
609 bizarre mosasaurid (Mosasauridae, Squamata) with shark-like cutting teeth from the upper
610 Maastrichtian of Morocco, North Africa. *Cretaceous Research* 123, 104764.

611 Longrich, N.R., Jalil, N.-E., Khaldoune, F., Yazami, O.K., Pereda-Suberbiola, X., Bardet, N., 2022.
612 *Thalassotitan atrox*, a giant predatory mosasaurid (Squamata) from the upper Maastrichtian phosphates
613 of Morocco. *Cretaceous Research* 140, 105315.

614 Marsh, O.C., 1869. ART. XXXIX.--Notice of some new Mosasauroid Reptiles from the Greensand of New
615 Jersey. *American Journal of Science and Arts (1820-1879)* 48, 392.

616 Mitkus, M., Potier, S., Martin, G.R., Duriez, O., Kelber, A., 2018. Raptor vision, Oxford research
617 encyclopedia of neuroscience.

618 Motani, R., Rothschild, B.M., Wahl Jr, W., 1999. Large eyeballs in diving ichthyosaurs. *Nature* 402, 747-
619 747.

620 Novas, F.E., Fernández, M.S., de Gasparini, Z.B., Lirio, J.M., Nuñez, H.J., Puerta, P., 2002. *Lakumasaurus*
621 *antarcticus*, n. gen. et sp., a new mosasaur (Reptilia, Squamata) from the Upper Cretaceous of
622 Antarctica.

623 Opper, M., 1811. Die ordnungen, familien und gattungen der reptilien als prodrom einer naturgeschichte
624 derselben. In commission bey J. Lindauer.

625 Páramo-Fonseca, M.E., 2013. *Eonatator coellensis* nov. sp.(Squamata: Mosasauridae), a new species
626 from the Upper Cretaceous of Colombia. *Revista de la Academia Colombiana de Ciencias Exactas, Físicas*
627 *y Naturales* 37, 499-518.

628 Polcyn, M.J., Jacobs, L.L., Araújo, R., Schulp, A.S., Mateus, O., 2014. Physical drivers of mosasaur
629 evolution. *Palaeogeography, Palaeoclimatology, Palaeoecology* 400, 17-27.

630 Polcyn, M.J., Lamb, J., 2012. The snout of *Halisaurus platyspondylus*: phylogenetic and functional
631 implications. *Bulletin de la Société Géologique de France* 183, 137-143.

632 Polcyn, M.J., Lindgren, J., Bardet, N., Cornelissen, D., Verding, L., Schulp, A.S., 2012. Description of new
633 specimens of *Halisaurus arambourgi* Bardet & Pereda Suberbiola, 2005 and the relationships of
634 Halisaurinae. *Bulletin de la Société Géologique de France* 183, 123-136.

635 Rempert, T.H., Martens, B.P., Melchers, A.P.V., 2022. First Record of a Tylosaurine Mosasaur from the
636 Latest Cretaceous Phosphates of Morocco. *Open Journal of Geology* 12, 883-906.

637 Rothschild, B., Martin, L., 2005. Mosasaur ascending: the phylogeny of bends. *Netherlands Journal of*
638 *Geosciences* 84, 341-344.

639 Russell, D., 1967. Systematics and morphology of American Mosasaurs (Reptilia, Sauria). *Bulletin of the*
640 *Peabody Museum of Natural History* 23, 1.

641 Schulp, A., Bardet, N., Bouya, B., 2009. A new species of the durophagous mosasaur *Carinodens*
642 (Squamata, Mosasauridae) and additional material of *Carinodens belgicus* from the Maastrichtian
643 phosphates of Morocco. *Netherlands Journal of Geosciences* 88, 161-167.

644 Schulp, A.S., Averianov, A.O., Yarkov, A.A., Trikolidi, F.A., Jagt, J.W., 2006. First record of the late
645 cretaceous durophagous mosasaur *Carinodens belgicus* (Squamata, Mosasauridae) from volgogradskaya
646 oblast'(Russia) and Crimea (Ukraine). Russian Journal of Herpetology 13, 175-180.
647 Schulp, A.S., Polcyn, M.J., Mateus, O., Jacobs, L.L., Morais, M.L., 2008. A new species of *Prognathodon*
648 (Squamata, Mosasauridae) from the Maastrichtian of Angola, and the affinities of the mosasaur genus
649 *Liodon*, Proceedings of the Second Mosasaur Meeting. Fort Hayes Studies, Special, pp. 1-12.
650 Strong, C.R., Caldwell, M.W., Konishi, T., Palci, A., 2020. A new species of longirostrine plioplatecarpine
651 mosasaur (Squamata: Mosasauridae) from the Late Cretaceous of Morocco, with a re-evaluation of the
652 problematic taxon '*Platecarpus' ptychodon*. Journal of Systematic Palaeontology 18, 1769-1804.
653 Tantawy, A., Keller, G., Adatte, T., Stinnesbeck, W., Kassab, A., Schulte, P., 2001. Maastrichtian to
654 Paleocene depositional environment of the Dakhla Formation, Western Desert, Egypt: sedimentology,
655 mineralogy, and integrated micro-and macrofossil biostratigraphies. Cretaceous Research 22, 795-827.
656 Watanabe, Y., Baranov, E.A., Sato, K., Naito, Y., Miyazaki, N., 2004. Foraging tactics of Baikal seals differ
657 between day and night. Marine Ecology progress series 279, 283-289.
658 Wiman, C., 1920. Some reptiles from the Niobrara Group in Kansas. Bulletin of the Geological Institution
659 of the University of Uppsala 18, 9-18.
660 Zdansky, O., 1934. The occurrence of mosasaurs in Egypt and in Africa in general. Bulletin de l'Institut
661 d'Egypte 17, 83-94.

662

663

664

665

666

667

668

670 **Table 1.** Described species of Halisaurinae.

Taxon	Synonymy	Stratigraphy	Location	Stage	References
<i>Eonatator sternbergii</i>	<i>Clidastes sternbergii</i> , <i>Halisaurus sternbergii</i>	Smoky Hill Member, Niobrara Chalk Formation	Kansas, United States	Santonian	Wiman, 1920; Bardet and Pereda- Suberbiola, 2001
<i>Halisaurus coellensis</i>	<i>Eonatator coellensis</i>	Nivel de Lutitas y Arenas	Tolima, Columbia	upper Campanian	Páramo-Fonseca, 2013
<i>Halisaurus ponpetelegans</i>	<i>Phosphorosaurus ponpetelegans</i>	Hakobuchi Formation	Hokkaido, Japan	lowermost Maastrichtian	Konishi et al., 2016
<i>Halisaurus platyspondylus</i>		New Egypt Formation	New Jersey, United States	upper Maastrichtian	Marsh, 1869; Polcyn and Lamb, 2012
<i>Halisaurus arambourgi</i>		Upper Couche III	Khouribga Province, Morocco	uppermost Maastrichtian	Bardet et al., 2005; Bardet 2012; Polcyn et al. 2012
<i>Halisaurus hebae</i>		Dakhla Shale	Western Desert, Egypt	lower Maastrichtian	This paper
<i>Phosphorosaurus ortliebi</i>	<i>Halisaurus ortliebi</i>	Ciply Phosphatic Chalk	Belgium	upper Maastrichtian	Dollo, 1889; Lingham-Soliar, 1996
<i>Pluridens walkeri</i>		Farin-Doutchi Formation	Niger	lower (?) Maastrichtian	Lingham-Soliar, 1998
<i>Pluridens calabaria</i>	<i>Pluridens walker</i>	Nkporo Shale	Nigeria	upper Campanian	Lingham-Soliar, 1998; Longrich, 2016
<i>Pluridens serpentis</i>		Upper Couche III	Khouribga Province, Morocco	uppermost Maastrichtian	Longrich et al.. 2021

672 **FIGURE CAPTIONS**

673

674 **Fig. 1.** Geological map of Dakhla area showing location of Gebel Gifata (modified after Abu El-
675 Kheir et al., 2022).

676

677 **Fig. 2.** Stratigraphic section of Gebel Gifata (modified after Abu El-Kheir et al., 2022).

678

679 **Fig. 3.** *Halisaurus hebae* sp. nov., NVP030, holotype, Gebel Gifata, Dakhla Oasis, Western
680 Desert (Egypt), lower Maastrichtian. Skull restoration (composite using bones from left and right
681 sides of the skull, only right maxilla shown reversed). Scale bar = 5 cm.

682

683 **Fig. 4.** *Halisaurus hebae* sp. nov., NVP030, holotype, Gebel Gifata, Dakhla Oasis, Western
684 Desert (Egypt), lower Maastrichtian, premaxilla, right maxilla and parts of left maxilla. A,
685 premaxilla in dorsal, B, ventral, and C, right lateral views; D, right maxilla in lateral and E,
686 medial views; F, left maxilla in lateral and G, medial views. Abbreviations: alv, dental alveolae;
687 fl, fluting; ib, internarial bar; rp, resorption pits. Scale bar = 5 cm.

688

689 **Fig. 5.** *Halisaurus hebae* sp. nov., NVP030, holotype, Gebel Gifata, Dakhla Oasis, Western
690 Desert (Egypt), lower Maastrichtian. Frontal in A, dorsal, B, ventral, C, left lateral and D,
691 posterior views. Abbreviations: ala, posterolateral ala; a-pof, articulation surface for
692 postorbitofrontal; a-prf, articulation surface for prefrontal; dff, descending flange of frontal; mdr,
693 median dorsal ridge; prsd, anterior parasagittal depression. Scale bar = 5 cm.

694

695 **Fig. 6.** Line drawing comparing halisaurine frontals. A, *Halisaurus platyspondylus* (redrawn
696 from Holmes & Sues, 2000-fig.1); B, *Halisaurus arambourgi* (redrawn from Polcyn et al., 2012-
697 fig.1.A); C, *Halisaurus ponpetelegans* (redrawn from Konishi et al., 2016-fig.7.A); D,
698 *Halisaurus hebae*; E, *Halisaurus coellensis* (redrawn from Paramo-Fonseca, 2013-fig.7.B); F,
699 *Eonatator sternbergii* (redrawn from Bardet & Pereda Suberbiola, 2001-fig.2.A); G,
700 *Phosphorosaurus ortliebi* (redrawn from Lingham-Soliar, 1996-fig.1.B); H, *Pluridens serpentis*
701 (redrawn from Longrich et al. 2021a, fig.5). Scale bar = 10 cm.

702

703 **Fig. 7.** *Halisaurus hebae* sp. nov. NVP030, holotype, Gebel Gifata, Dakhla Oasis, Western
704 Desert (Egypt), lower Maastrichtian. Parietal in A, dorsal, B, ventral, and C, left lateral views.
705 Scale bar = 5 cm. Abbreviations: msr, midsagittal ridge; pf, parietal foramen; prsf, parasagittal
706 furrow; prsd, anterior parasagittal depression; ptb, parietal table; sr, suspensorial ramus.

707

708 **Fig. 8.** *Halisaurus hebae* sp. nov., NVP030, holotype, Gebel Gifata, Dakhla Oasis, Western
709 Desert (Egypt), lower Maastrichtian. Left jugal in A, lateral and B, medial views. Scale bar = 5
710 cm.

711

712 **Fig. 9.** *Halisaurus hebae* sp. nov., NVP030, holotype, Gebel Gifata, Dakhla Oasis, Western
713 Desert (Egypt), lower Maastrichtian. Left quadrate in A, anterior, B, posterior, C, lateral, D,
714 medial, E, dorsal and F, ventral views. Abbreviations: co, mandibular condyle; ist, infrastapedial
715 process; mr, median ridge of shaft; sst, suprastapedial process; ta, tympanic ala; tc, tympanic
716 crest; tm, tympanic meatus. Scale bar = 5 cm.

717

718 **Fig. 10.** *Halisaurus hebae* sp. nov., NVP030, holotype, Gebel Gifata, Dakhla Oasis, Western
719 Desert (Egypt), lower Maastrichtian. Braincase in A, ventral, B, dorsal, C, posterior and D, left
720 dorsolateral views. Abbreviations: Bocc, basioccipital; Bsph, basisphenoid; bs-bo, basisphenoid-
721 basioccipital suture; bt, basal tubera of basioccipital; oc, basioccipital condyle; Op, opisthotic;
722 op-pro, opisthotic-prootic suture; popr, paroccipital process of the opisthotic; Pro, prootic; Socc,
723 supraoccipital; St, supratemporal. Scale bar = 5 cm.

724

725 **Fig. 11.** *Halisaurus hebae* sp. nov., NVP030, holotype, Gebel Gifata, Dakhla Oasis, Western
726 Desert (Egypt), lower Maastrichtian. Bones of the left mandibular ramus, A, dentary in lateral, B,
727 medial views; C, splenial in lateral and D, ventral views; E, coronoid in lateral and F, medial
728 views; G, angular in medial view; H, surangular in lateral, I, dorsal and J, medial views.
729 Abbreviations: af, adductor fossa; Art, articular; co, angular condyle; ct, splenial cotyle; f,
730 dentary foramina; gf, glenoid fossa; mc, Meckelian canal; prp, prearticular process of the
731 articular; rp, retroarticular process of the articular; Sur, surangular. Scale bar = 5 cm.

732

733 **Fig. 12.** *Halisaurus hebae* sp. nov., NVP030, holotype, Gebel Gifata, Dakhla Oasis, Western
734 Desert (Egypt), lower Maastrichtian. Closeup showing the large contribution of the surangular to
735 the glenoid fossa, in A, medial and B, dorsal views. Scale bar = 5 cm

736

737 **Fig. 13.** *Halisaurus hebae* sp. nov., NVP030, holotype, Gebel Gifata, Dakhla Oasis, Western
738 Desert (Egypt), lower Maastrichtian. Closeup showing teeth, in A, some isolated teeth; B, in the
739 maxilla.

740

741 **Fig. 14.** *Halisaurus hebae* sp. nov., NVP030, holotype, Gebel Gifata, Dakhla Oasis, Western
742 Desert (Egypt), lower Maastrichtian, anterior vertebrae, A, Axis vertebra in lateral and B,
743 posterior views. Other selected cervical vertebrae; in D, anterior view, in C and E, posterior
744 view. Selected dorsal vertebra; in F, anterolateral view and G, posterior view. Abbreviations: co,
745 condyle; ct, cotyle; hyp, hypapophysis; ns, neural spine; poz, postzygapophysis; prz,
746 prezygapophysis; syn, synapophysis. Scale bar = 5 cm.

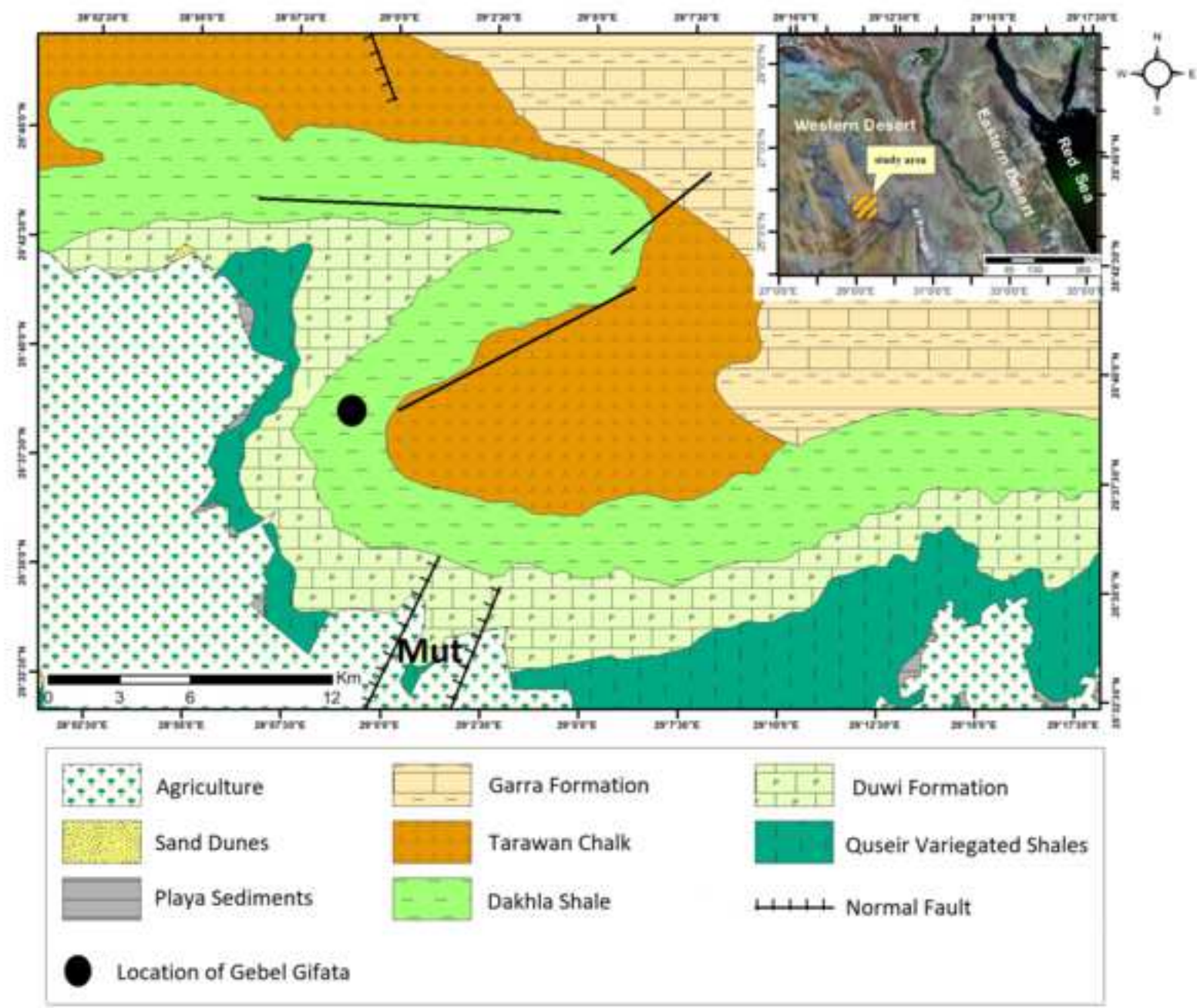
747

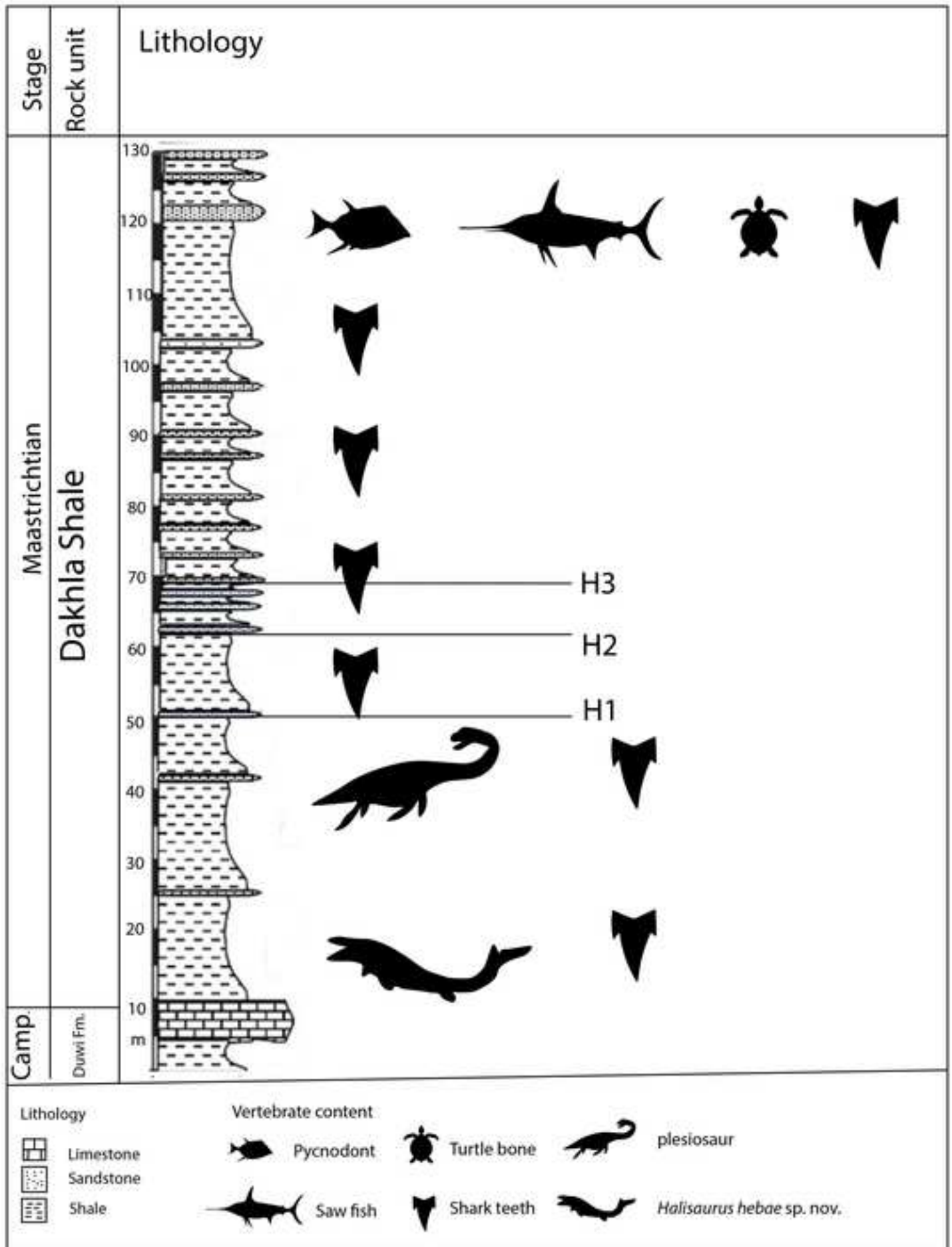
748 **Fig. 15.** Phylogeny showing the relationships of *Halisaurus hebae* sp. nov.

749

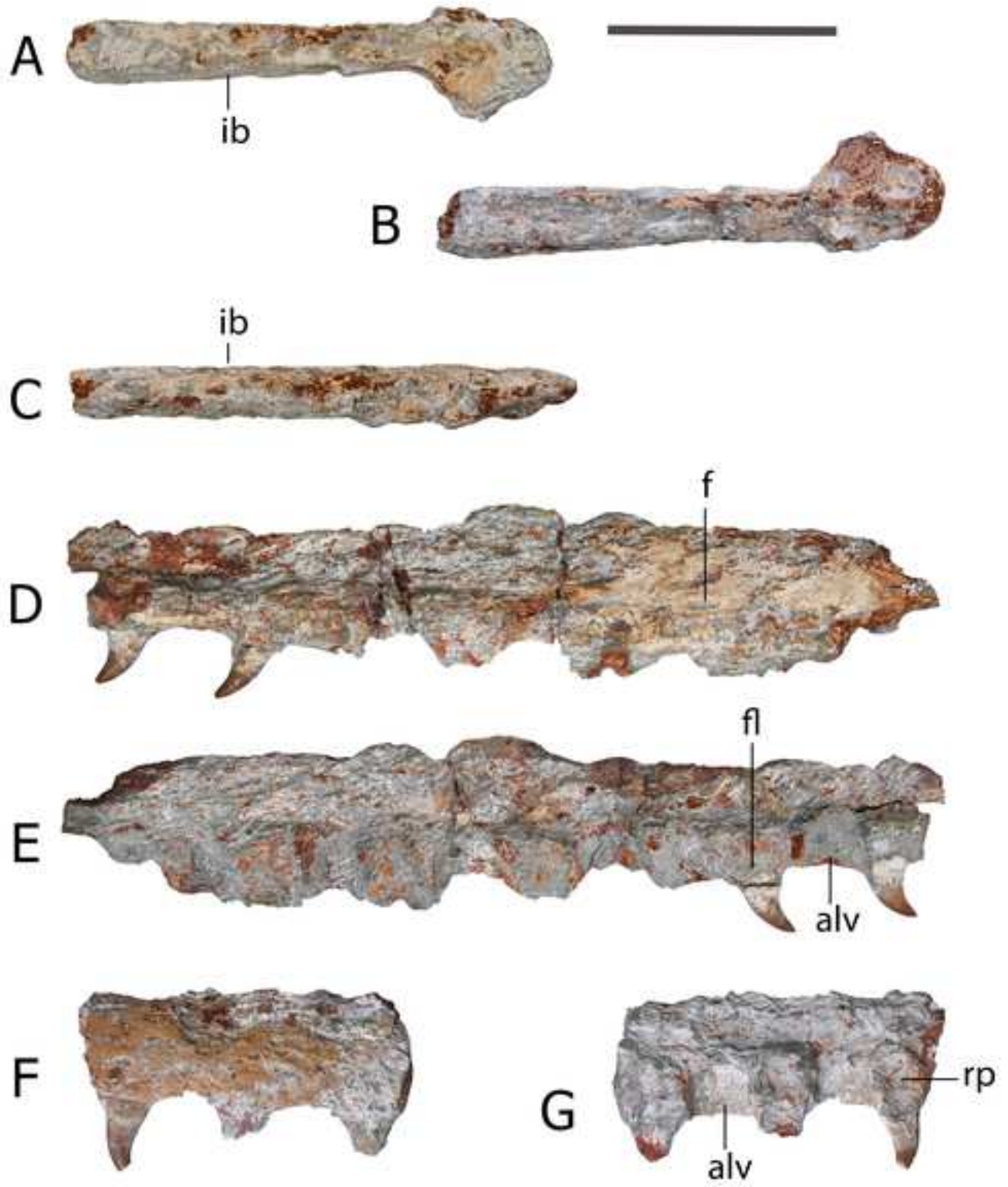
750 **Fig. 16.** Silhouette showing the relative size of *Halisaurus hebae* sp. nov.

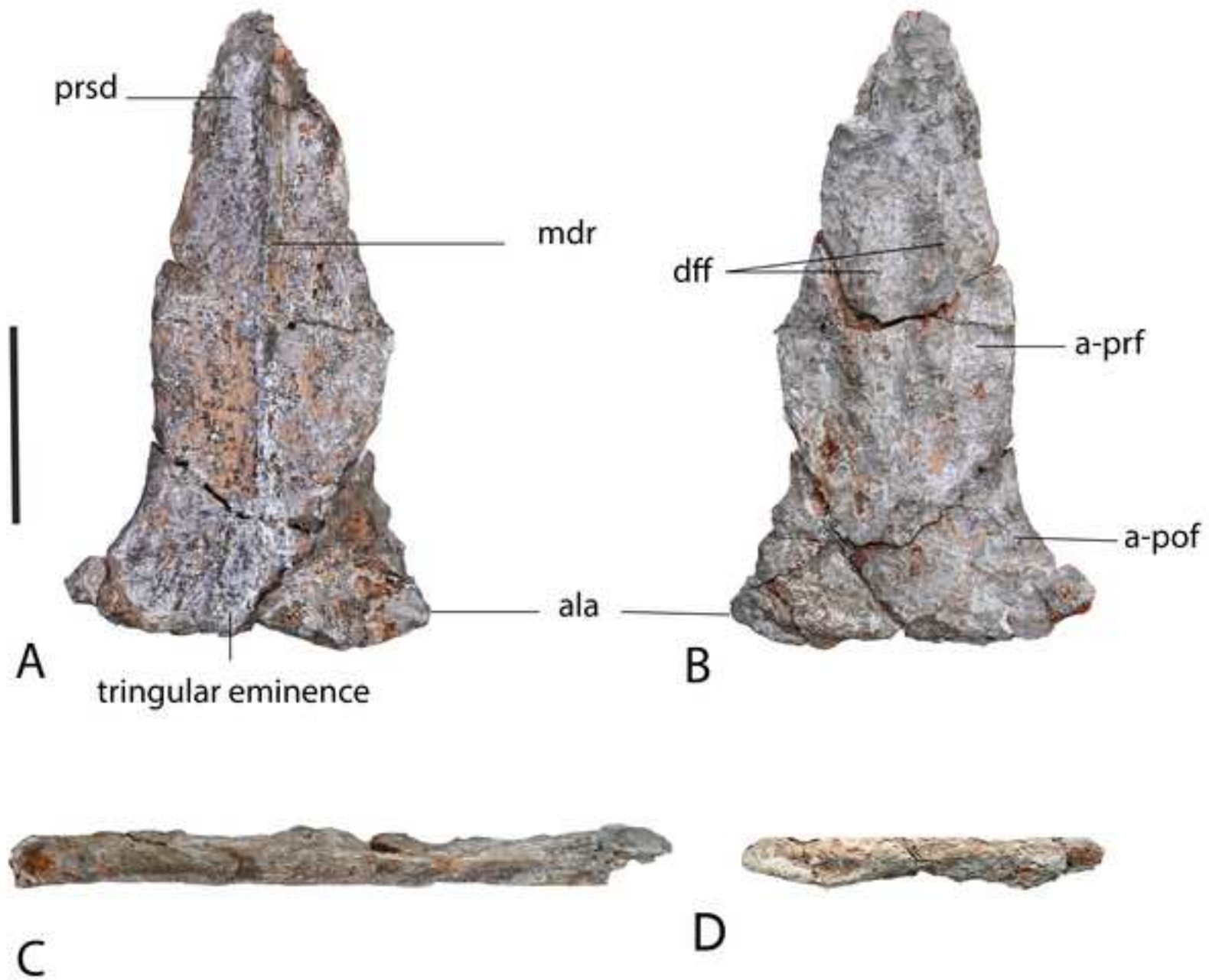
Figure 1

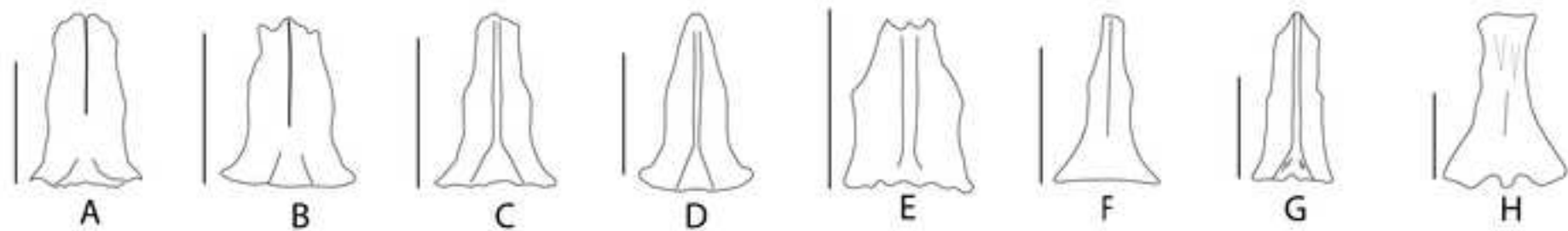


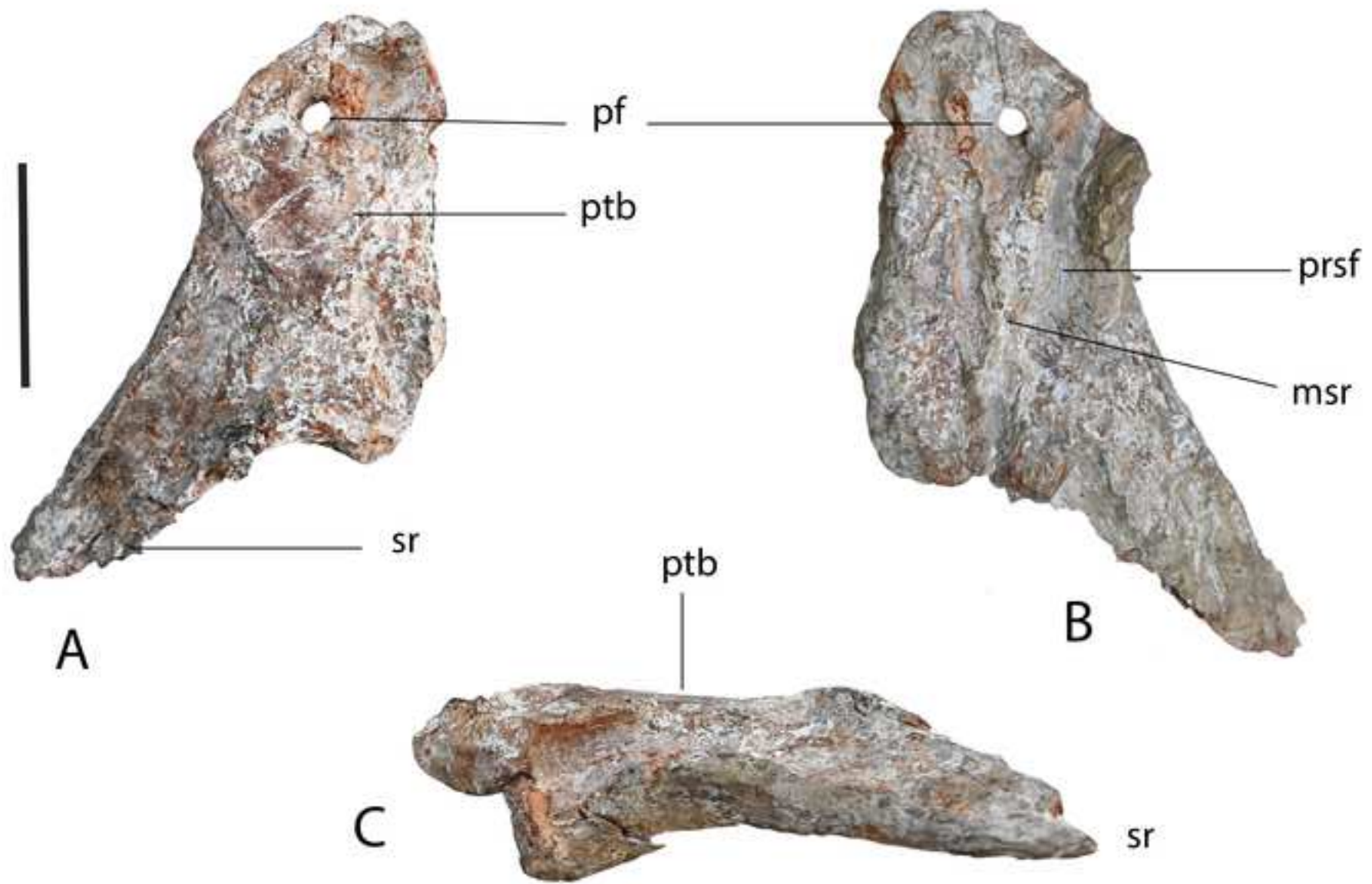










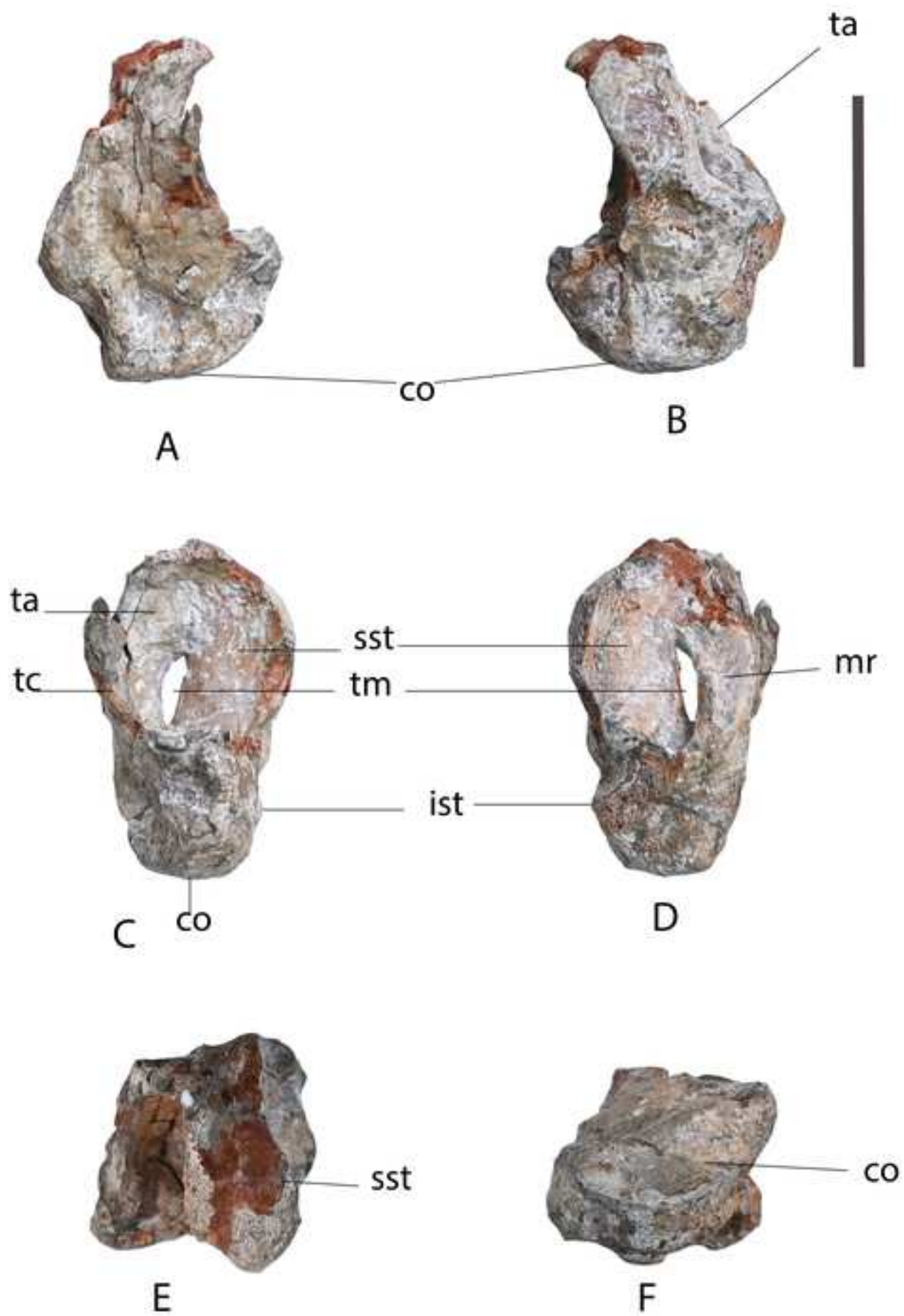


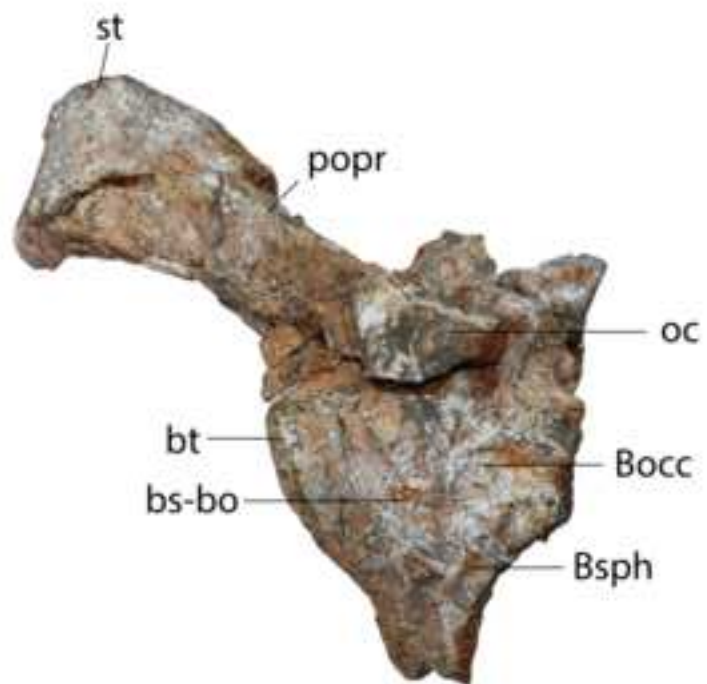


A

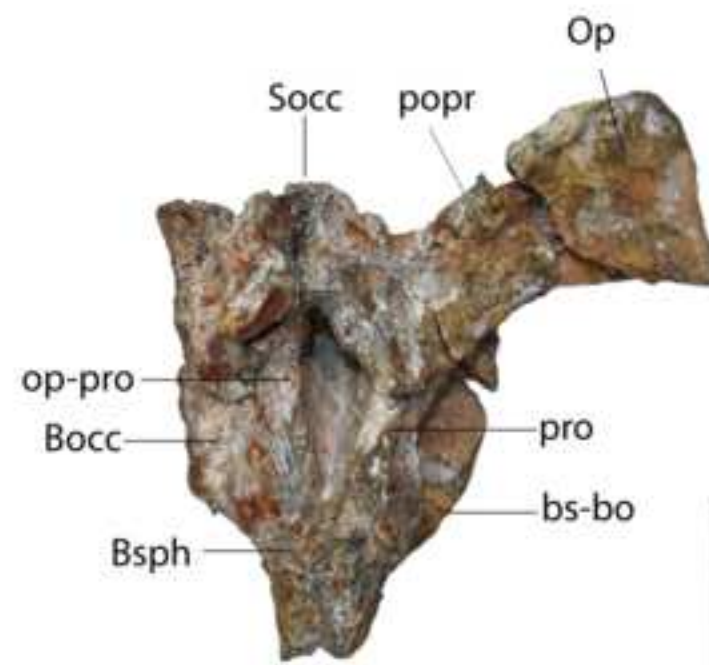


B

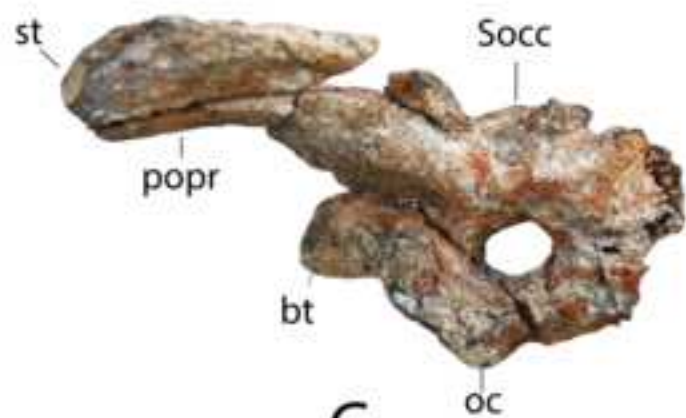




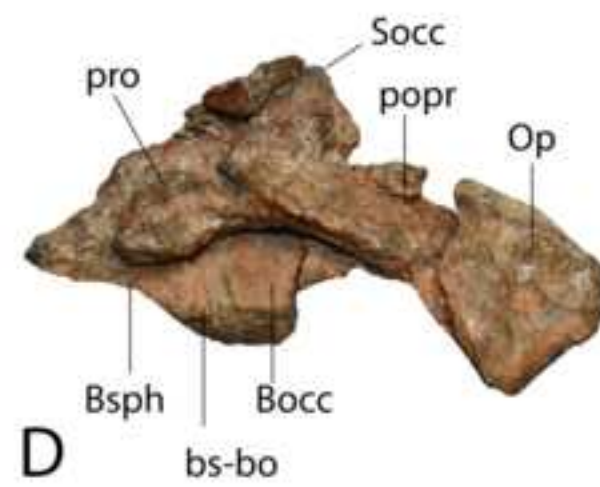
A



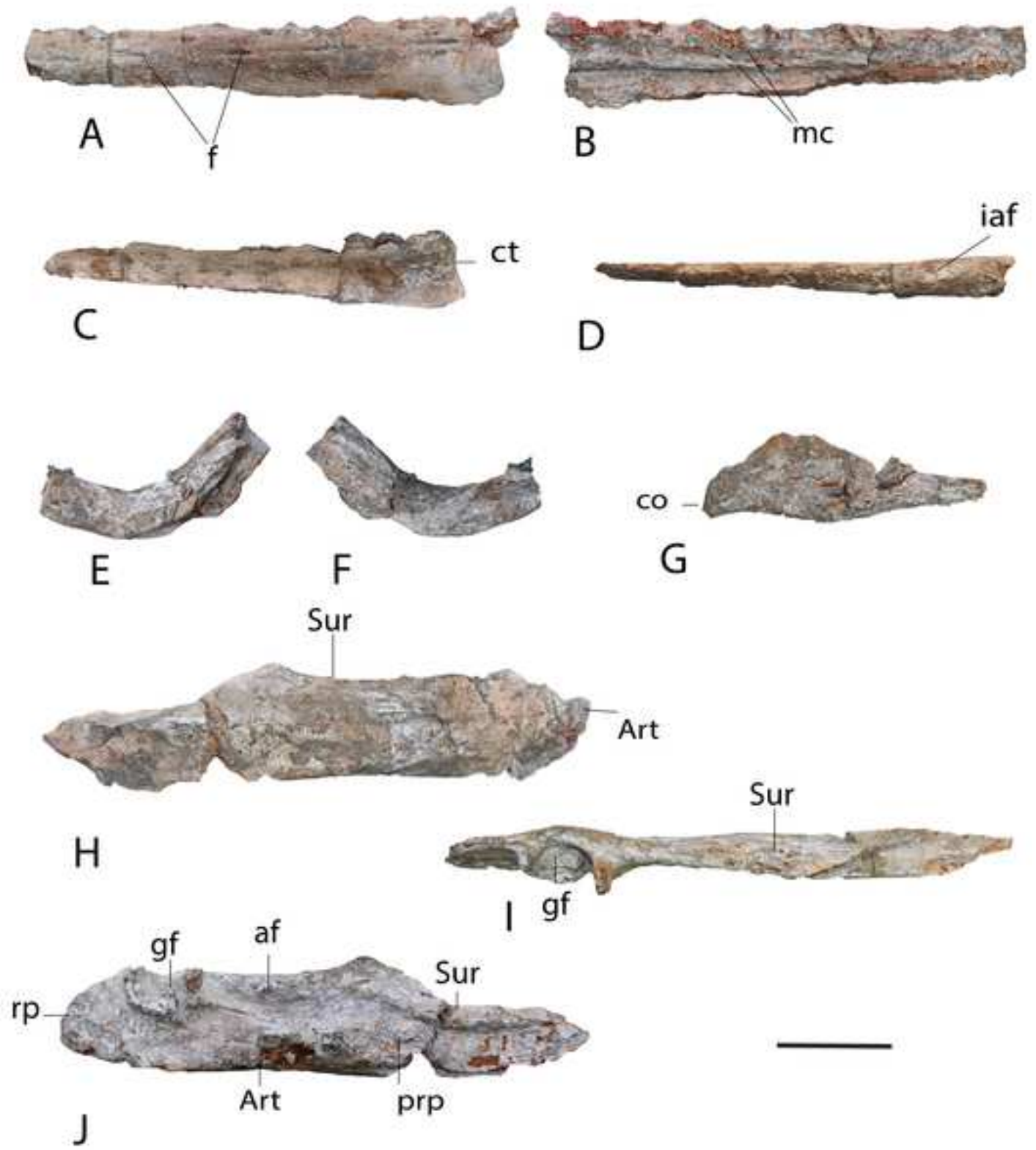
B



C



D







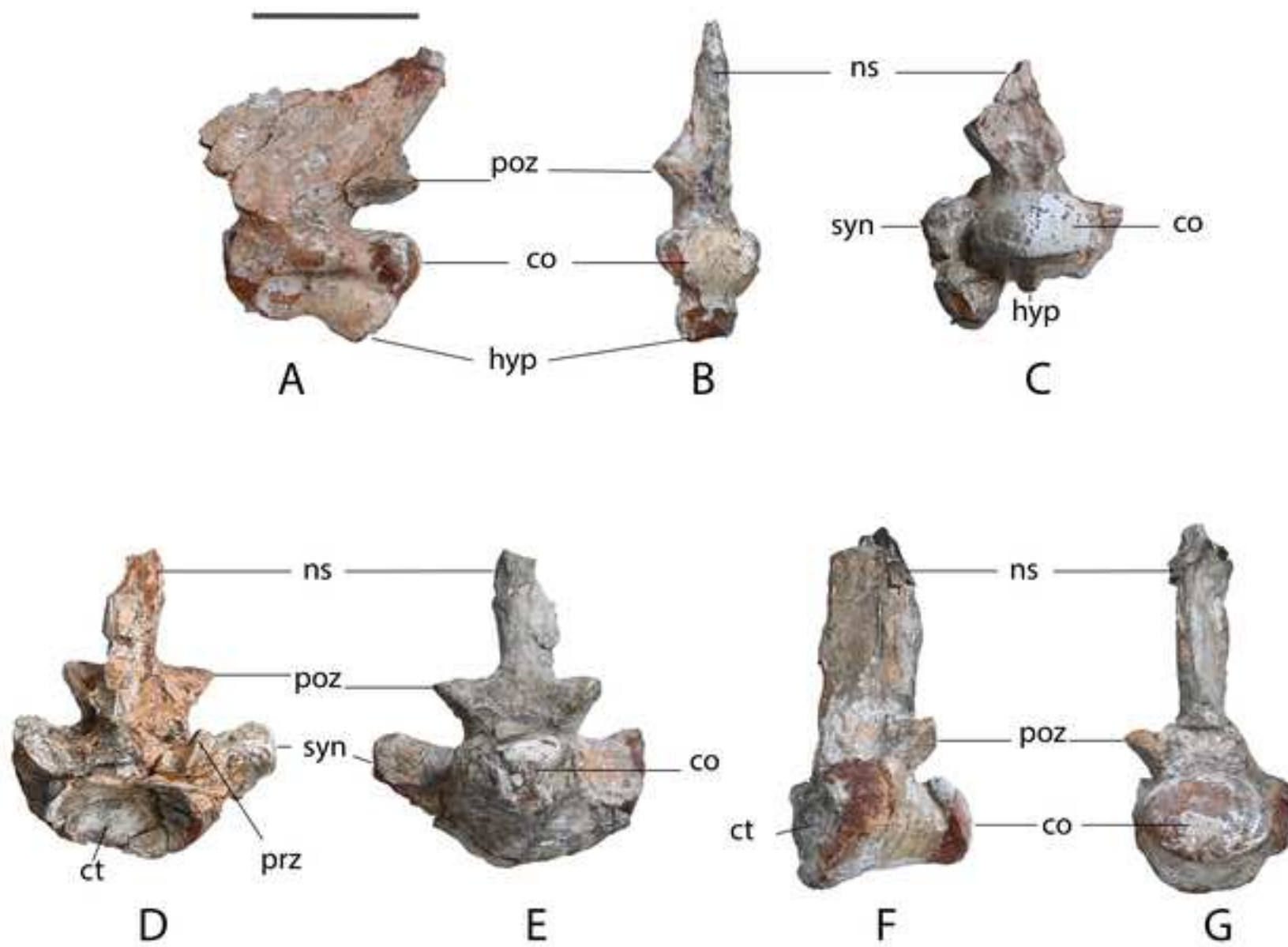


Figure 15

